Emergence of Supercoiling-Mediated Regulatory Networks through the Evolution of Bacterial Chromosome Organization

Théotime Grohens[1] Sam Meyer[2]
Guillaume Beslon[3,*]

[1]Centre for Genomic Regulation, Barcelona Institute of Science and Technology, Dr. Aiguader 88, Barcelona 08003, Spain
[2]Université de Lyon, INSA Lyon, Université Claude Bernard Lyon 1, CNRS, UMR5240 MAP, F-69622, France
[3]Université de Lyon, INSA Lyon, Inria, ECL, Université Claude Bernard Lyon 1, Université Lumière Lyon 2, CNRS, LIRIS UMR 5205, F-69622, France
*Corresponding author: guillaume.beslon@insa-lyon.fr

Abstract

DNA supercoiling – the level of twisting and writhing of the DNA molecule around itself – plays a major role in the regulation of gene expression in bacteria by modulating promoter activity. The level of DNA supercoiling is a dynamic property of the chromosome, which varies both at local and global scales, in response to external factors such as environmental perturbations and to internal factors including gene transcription. As such, local variations in supercoiling could in theory couple the expression levels of neighboring genes by creating feedback loops between their transcription rates. However, the impact of such supercoiling-mediated interactions on the regulation of gene expression remains uncertain. In this work, we study how this coupling between transcription and supercoiling could shape genome organization and help regulate gene transcription. We present a model of genome evolution in which individuals whose gene transcription rates are coupled to supercoiling must adapt to two environments that induce different global supercoiling levels. In this model, we observe the evolution of whole-genome regulatory networks that provide control

over gene expression by leveraging the transcription-supercoiling coupling, and show that the structure of these networks is underpinned by the organization of genes along the chromosome at several scales. Local variations in DNA supercoiling could therefore help jointly shape both gene regulation and genome organization during evolution.

1 Introduction

DNA is the material basis of genetic information. It is a flexible polymer comprising two strands of nucleotides that coil around each other. In the cell, DNA is subject to torsional stress, inducing what is known as DNA supercoiling in the form of twist (deformation around the helical axis) and writhe (3D deformation of the helical axis). The level of supercoiling σ is an important physiological parameter, and it is measured in a given DNA molecule as the relative difference between its linking number (the number of times its strands cross each other, which is affected by twist and writhe) and that of a relaxed DNA molecule of the same length. In bacteria, DNA is normally maintained in a negatively supercoiled state, with a typical value of $\sigma_{basal} = -0.06$ in *Escherichia coli* (Travers and Muskhelishvili, 2005). In these organisms, DNA supercoiling is an important regulator of gene expression, as changes in the level of supercoiling directly affect gene transcription rates (Jovanovich and Lebowitz, 1987; Peter et al., 2004; Dorman and Dorman, 2016).

Regulation of DNA Supercoiling In bacteria, the level of DNA supercoiling is primarily controlled by topoisomerases, enzymes that alter supercoiling by passing DNA through single- or double-strand breaks. The two main topoisomerases are gyrase, which introduces negative supercoils at an ATP-dependent rate, and topoisomerase I, which oppositely relaxes negative supercoiling without ATP (Champoux, 2001). The average chromosomal supercoiling level depends on their relative activity, and changes depending on the environmental conditions. A prime example can be found in *E. coli*, where DNA is more negatively supercoiled during exponential growth, and more relaxed in stationary phase (Travers and Muskhelishvili, 2005). Supercoiling also responds to environmental stresses: salt shock causes a transient increase in negative DNA supercoiling in *E. coli* (Hsieh et al., 1991); an acidic intracellular environment causes DNA relaxation in the facultative pathogen *Salmonella enterica* var. Typhimurium (Marshall et al., 2000); and higher temperatures also relax DNA in the plant pathogen *Dickeya dadantii* (Hérault et al., 2014). These responses are usually very well conserved among species (Martis B. et al., 2019), and the level of supercoiling therefore constitutes a global

regulatory parameter subject to cellular control. Moreover, supercoiling does not only vary through time, but also depending on chromosomal location. In particular, according to the *twin-domain* model of supercoiling presented in Liu and Wang (1987), the transcription of a gene by an RNA polymerase generates both positive supercoils downstream and negative supercoils upstream of the transcribing polymerase (Guo et al., 2021; Sutormin et al., 2022; Visser et al., 2022), as a consequence of the drag that hampers the rotation of the transcriptional complex (polymerase, RNA, and associated ribosomes and proteins) around DNA during transcription. Furthermore, while the intrinsic flexibility of the DNA polymer allows supercoils to diffuse along the chromosome, physical constraints induced by the 3D confinement of the nucleoid and by DNA-bound proteins form topological obstacles and barriers that block its diffusion (Postow et al., 2004; Deng et al., 2004; Junier et al., 2023). As a result, bacterial chromosomes are estimated to be partitioned in topological domains with an average size of 10 kb (Postow et al., 2004).

Global Regulatory Role of DNA Supercoiling The level of DNA supercoiling influences gene expression in bacteria through several mechanisms (Jovanovich and Lebowitz, 1987; Peter et al., 2004; Dorman and Dorman, 2016). In particular, more negatively supercoiled DNA facilitates the initiation of gene transcription, as opening the DNA double strand – the initial step of gene transcription – is thermodynamically favored in more negatively supercoiled DNA regions (El Houdaigui et al., 2019). In *E. coli*, Peter et al. (2004) showed that 7% of genes were either up- or down-regulated by a global relaxation (a less negative supercoiling level) of chromosomal DNA. Similar transcriptional responses to DNA relaxation were obtained for *S. enterica* (Webber et al., 2013), and for *S. pneumoniae* (Ferrandiz et al., 2010), and to an increase in negative supercoiling in *D. dadantii* (Pineau et al., 2022). In this bacteria, the chromosome consists in domains that exhibit markedly different supercoiling and transcriptional responses to environmental stresses (Muskhelishvili et al., 2019), suggesting that supercoiling could mediate the expression of pathogenic genes in stressful environments.

DNA supercoiling might play an especially important regulatory role in bacteria with reduced genomes, such as the obligate aphid endosymbiotic bacterium *Buchnera aphidicola*. As *B. aphidicola* is nearly devoid of transcription factors, global and local changes in supercoiling are thought to be one of the main mechanisms available to this bacteria for the regulation of gene expression (Brinza et al., 2013). In *Mycoplasma pneumoniae*, another genome-reduced bacterium, other work has also shown that supercoiling plays a global regulating role, and that it might mediate transcriptional interference between convergent genes (Yus et al., 2019). Finally, mutations that alter the regulation of DNA

supercoiling have also been shown to be evolutionarily favorable in experimental settings. For example, in the so-called *Long-Term Evolution Experiment*, 12 populations of *E. coli* cells seeded from a common ancestor have been adapting to a laboratory environment for over 75,000 generations (Lenski et al., 1991; Lenski, 2023). In this experiment, 10 out of the 12 populations were shown to present a higher level of negative supercoiling relative to their ancestor, with one population in particular presenting an increase of more than 17% in negative supercoiling (Crozat et al., 2005). In this population, two distinct mutations were shown to increase negative supercoiling when inserted back into the ancestral strain, and to provide a significant growth advantage (that is, higher fitness) relative to the ancestral strain. This evolutionary trajectory was then shown to be repeatable not only at the phenotypic level, but also at the genetic level, with a majority of strains harboring mutations in DNA supercoiling-related genes (Crozat et al., 2010). In the context of the *LTEE*, supercoiling mutations therefore played a role in the adaptation of *E. coli* strains to new environments, evidencing the important effect of DNA supercoiling on bacterial gene regulation.

The Transcription-Supercoiling Coupling When two genes are located closely enough on the genome, the supercoiling generated by the transcription of one gene can in theory affect the transcription level of the other gene, and vice versa. This interaction has long been been suspected to play a regulatory role (Pruss and Drlica, 1989; Lilley et al., 1996), and, following Meyer and Beslon (2014), we will refer to it as to the *transcription-supercoiling coupling*. This coupling can take several forms depending on the relative orientation of the genes: divergent genes could increase their respective transcription level in a positive feedback loop; convergent genes could inhibit the transcription of one another; and, in tandem genes, the transcription of the downstream gene could increase the transcription of the upstream gene, and the transcription of the upstream gene decrease the transcription of the downstream gene.

Such supercoiling-mediated interactions between neighboring genes have been experimentally documented in several bacterial genetic systems. In the *E. coli*-related pathogen *Shigella flexneri*, the *virB* promoter is normally only active at high temperatures, but can be activated at low temperatures by the insertion of a phage promoter in divergent orientation (Tobe et al., 1995). Similarly, the expression of the *leu-500* promoter in *S. enterica* can be increased or decreased by the insertion of upstream transcriptionally active promoters, depending on their orientation relative to *leu-500* (El Hanafi and Bossi, 2000). The transcription-supercoiling coupling has also been explored in a synthetic construct in which the inducible *ilvY* and *ilvC* *E. coli* promoters were inserted on a plasmid in divergent orien-

tations (Rhee et al., 1999). In that system, a decrease in the activity of *ilvY* was associated with a decrease in *ilvC* activity, and an increase in *ilvY* activity with a corresponding increase in *ilvC* activity. However, recent work in *E. coli* has shown that supercoiling, and in particular polymerase-generated supercoiling, does not only impact transcription initiation but also transcription speed, resulting in lower expression of a target gene through slower transcription when a divergently oriented gene was induced in a synthetic plasmid (Kim et al., 2019).

The biological relevance of the transcription-supercoiling coupling might however not be limited to such local interactions. Indeed, in *E. coli*, the typical size of topological domains – inside which the positive and negative supercoils generated by gene transcription can propagate – is usually estimated to range around 10 kb (Postow et al., 2004), and transcription-generated supercoiling has been shown to propagate up to 25 kb in each direction around some specific genes (Visser et al., 2022). As genes stand on average 1 kb apart on the *E. coli* chromosome (Blattner, 1997), any single topological domain could therefore encompass multiple genes interacting via the transcription-supercoiling coupling. Supercoiling-sensitive genes have indeed been shown to group in local up- or down-regulated clusters, found all around the chromosome, in bacteria such as *E. coli* (Peter et al., 2004), *S. enterica* (Webber et al., 2013) and *S. pneumoniae* (Ferrandiz et al., 2010). Focusing on *E. coli*, a statistical analysis of the relative position of neighboring genes on the chromosome of this bacteria indeed showed that genes that are up-regulated by negative supercoiling have more neighbors in divergent orientations, while genes that are down-regulated by negative supercoiling have more neighbors in converging orientations (Sobetzko, 2016). The co-localization of genes in such clusters has therefore been hypothesized to play a phenotypic role by enabling a common regulation of their transcription through local variations in the supercoiling level. Finally, synteny segments – clusters of neighboring orthologous genes that show correlated expression patterns – have been shown to be more conserved than expected by chance in a study considering over 1,000 bacterial species, including in particular the distantly related *E. coli* and *Bacillus subtilis*, possibly as a consequence of co-regulation of the genes within these segments through supercoiling (Junier and Rivoire, 2016). Overall, this body of empirical evidence suggests that local variations in the supercoiling level, due to its coupling with transcription, could indeed play a substantial role in the regulation of gene activity and consequently impact the evolution of genome organization.

Multiple modeling works have recently addressed the simulation of the transcription-supercoiling coupling, reporting contrasted results (El Houdaigui et al., 2019; Geng et al., 2022; Sevier and Hor-

moz, 2022; Johnstone and Galloway, 2022; Boulas et al., 2023). Quantitative regulatory rules that result from this coupling thus still remain to be fully characterized. Here, we address a different question that has never been subject to detailed analysis: how the transcription-supercoiling coupling may drive genome evolution. We present a two-level framework, in which a whole-genome model of the transcription-supercoiling coupling is embedded within an evolutionary simulation. The regulatory aspect of the model is voluntarily kept simple, assuming that local negative supercoils always activate gene expression. In this framework, individuals must evolve gene expression levels that are adapted to two environments, characterized by different global supercoiling levels, using chromosomal rearrangements only. We first show that complex environment-driven patterns of gene expression are able to evolve in such a model, observing in particular the emergence of relaxation-activated genes. We then characterize the spatial organization of genes along the genome that is responsible for these expression patterns in the model, showing that genes are locally organized in patterns which leverage the transcription-supercoiling coupling for either activation or inhibition, such as toggle switches, but that larger-scale networks are required to strongly inhibit genes. Finally, we show that, in our model, genes form a densely connected genome-wide interaction network, overall demonstrating that supercoiling-based regulation could indeed coevolve with genome organization in bacterial genomes.

2 Results

2.1 Evolution of Gene Regulation through the Transcription-Supercoiling Coupling

We introduce a model (detailed in the Methods section) in which populations of individuals must evolve to adapt their gene expression levels to two different environments during their life. In the model, individuals are described by a circular genome containing a constant number of genes, placed at different positions and orientations along the genome. The main assumptions of the model are that the expression level of a gene only depends on the local level of supercoiling at the location of its promoter, and that this local supercoiling level itself only depends on the following elements: the basal level of supercoiling of the chromosome, a constant perturbation of this level in each environment, and the transcription rate of neighboring genes, with a magnitude linearly decreasing with the distance to the transcribed gene (see Equations 1 to 4 in Methods). Moreover, we assume that gene transcription and DNA supercoiling are continuous functions of one another, and we assume that they always reach

a deterministic equilibrium state. We can thus define, for a given individual in a given environment, a unique expression level for each gene and a unique level of supercoiling at every genome position. These assumptions allow us to compute the fitness of all individuals as a function of the difference between their computed and expected gene expression levels in each environment. Finally, we use this fitness to choose reproducers in order to create a new population at every generation of the simulation.

The two environments used in the simulation are characterized by their respective impact $\delta\sigma_{env}$ on the background supercoiling level of the chromosome of each individual. The first environment, named environment A, induces a global relaxation of DNA as in the acidic macrophage vacuoles encountered by *S. enterica* (Marshall et al., 2000). In the model, we consider that this relaxation decreases baseline gene expression ($\delta\sigma_{env} = \delta\sigma_A = 0.01$). The second environment, named environment B, oppositely induces an increase in negative DNA supercoiling, as observed for example when shifting *E. coli* cultures to a salt-rich medium (Hsieh et al., 1991). In the model, we consider this negative supercoiling to oppositely increase baseline gene expression ($\delta\sigma_{env} = \delta\sigma_B = -0.01$). These environments could also be considered to reflect the stationary phase of *E. coli*, in which DNA is more relaxed, versus the exponential growth phase in which it is more negatively supercoiled (Travers and Muskhelishvili, 2005). In order to have high fitness, individuals must display environment-specific gene expression patterns, obtained by the activation or inhibition of three disjoint subsets of their genes – called A, B and AB – in each environment: A genes must be activated in environment A but not in environment B, B genes in environment B but not in environment A, and AB genes must be activated in both environments. At every generation of the simulation, we compute the fitness of every individual based on their gene expression levels in each of these environments, then create the next generation by making individuals reproduce proportionally to their fitness, and applying random mutations to their offspring. Importantly, as we focus on the evolution of genome organization, the only mutational operator that we use is genomic inversions, which can reorder genes on the genome, thereby affecting gene expression levels and hence fitness.

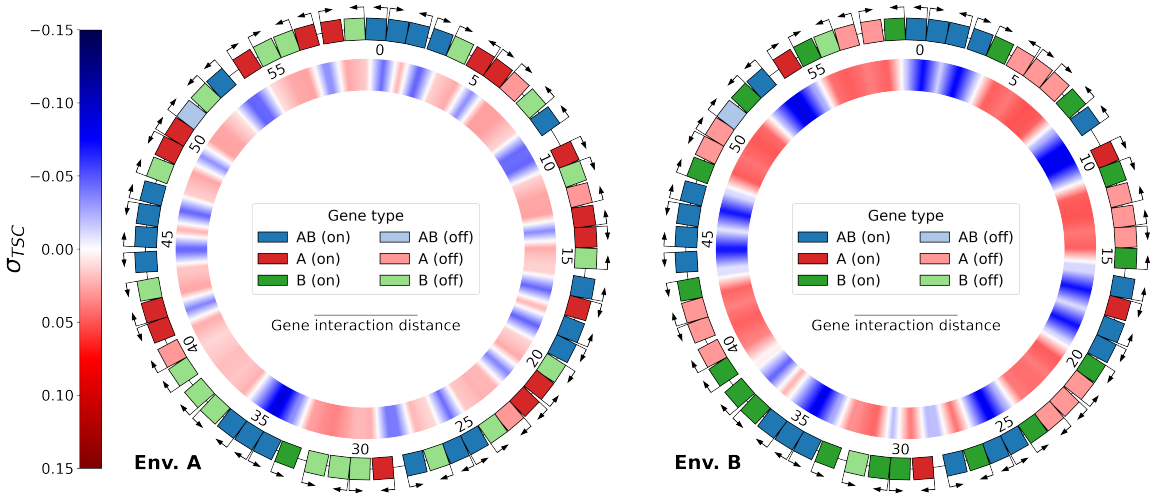

Figure 1: Genome of the best individual at the last generation of evolution of replicate 21, evaluated in the two environments: A (relaxed DNA, left) and B (more negatively supercoiled DNA, right). The outer ring shows the type, orientation, and expression of each gene on the genome (darker color: activated; lighter color: inhibited). Genes are considered to be activated if their expression is above the threshold $e_{1/2}$, and inhibited otherwise (see Methods). Genes are numbered clockwise according to their position on the genome. The inner ring shows the level of transcription-generated DNA supercoiling σ_{TSC} at every position on the genome. Shades of blue represent negative supercoiling ($\sigma_{TSC} < 0$), and shades of red positive supercoiling ($\sigma_{TSC} > 0$).

Evolution of Environment-Specific Gene Expression Levels Using the model presented above, we let 30 populations of 100 individuals, each possessing 20 genes of each type for a total of 60 genes, evolve for 1,000,000 generations. The genome of a typical individual at the end of the evolutionary simulation is depicted in Figure 1, in environments A (left) and B (right). In each case, the outer ring depicts gene position, orientation, type, and activation, and the inner ring the local level of supercoiling due to gene transcription σ_{TSC}. We consider that a gene is activated if its expression is above the expression threshold $e_{1/2}$, and inhibited otherwise (see Methods). In this individual's genome, different activation patterns are visible, for each gene type and as a function of the environment. All the AB genes except one (gene 51) are correctly activated (dark blue) in the two environments; 19 out of 20 B genes are correctly inhibited (light green) in environment A (left) while 18 are correctly activated (dark green) in environment B (right); and 16 A genes are activated (dark red) in environment A, while 16 are inhibited (light red) in environment B. Note that this asymmetry between the number of A and B genes that are in the expected state is due to an asymmetry in the effect of the environments themselves, which we will discuss below in more detail.

The transcription-generated supercoiling that is represented in the inner ring can also be seen to

change consistently with the gene activation patterns between the two environments: zones of negative DNA supercoiling (in blue) are delineated by divergently oriented activated genes, while zones of positive DNA supercoiling (in red) contain inhibited genes. The genome of this evolved individual therefore shows that, in the context of this model, it is possible for evolution to adjust gene expression levels to an environment-dependent target solely by rearranging relative gene positions and leveraging the transcription-supercoiling coupling between neighboring genes.

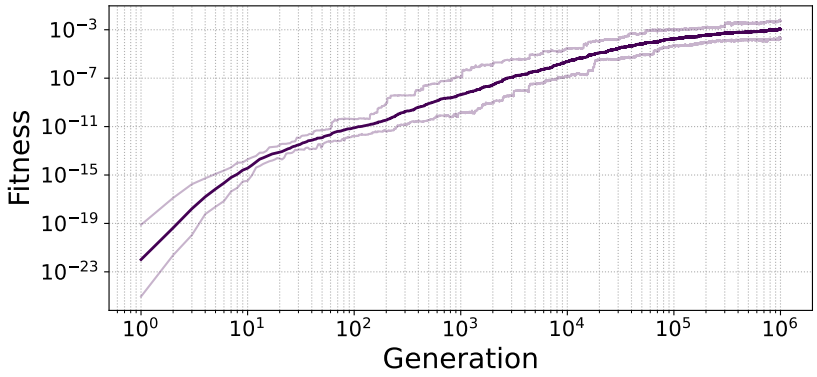

Figure 2: Geometric average of the fitness of the best individual in each of the 30 populations, at every generation. Lighter lines represent the first and last decile of the data.

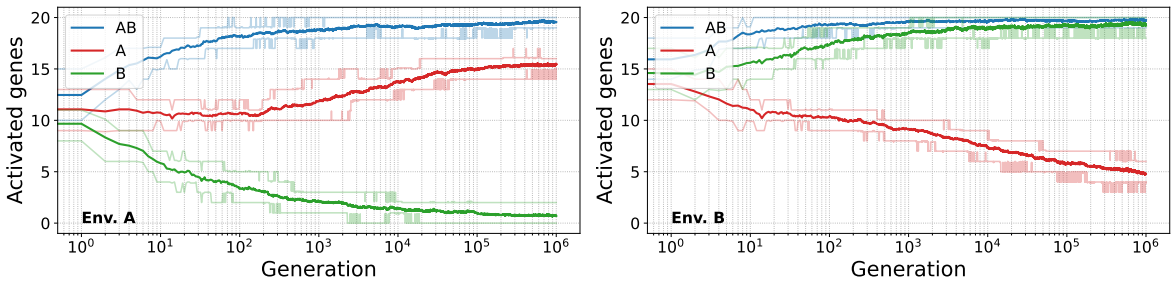

Figure 3: Average number of activated genes (expression higher than $e_{1/2}$) of each type in the best individual at every generation, averaged over the 30 populations, in environments A (left) and B (right). Lighter lines represent the first and last decile of the data.

This behavior is however not specific to this particular individual. Figure 2 shows that the fitness of the best individual of each population, averaged over all populations, evolves smoothly towards higher values over the course of the simulation. More precisely, Figure 3 shows that the numbers of activated genes of each particular type also evolve towards their respective targets, in environment A (left) and B (right). In each environment, the average number of activated AB genes (in blue) quickly reaches nearly 20, its maximum value, as expected from their target; B genes (in green) show the

same behavior, evolving towards nearly full activation in environment B and nearly full inhibition in environment A. A genes (in red) follow a slightly different course, as the number of activated A genes seems to converge to approximatively 15 out of the expected 20 in environment A, but continues to decrease towards the expected 0 in environment B by the end of the simulations.

The incomplete match of A genes with their evolutionary target – as compared to B genes – could however be partially expected. Environment A is indeed characterized by a *less negative* global supercoiling level, while environment B is characterized by a *more negative* global supercoiling level (recall that the basal supercoiling level is negative). As less negative supercoiling reduces gene transcription, it is by construction more difficult for a gene to have a high transcription rate in environment A than in environment B. A genes must therefore complete the more difficult task of being activated in the inhibiting environment A, while being inhibited in the activating environment B, whereas B genes must complete the comparatively easier task of being activated in the "easier" environment B and inhibited in the "harder" environment A.

Well-differentiated expression levels nonetheless do evolve in our model for both types of genes, in response to the different supercoiling levels imposed by the environmental conditions. These gene expression patterns are moreover remarkably robust to the magnitude of the difference between the environments. Indeed, we still observe such patterns even when repeating the experiment with environmental perturbations 10 and 100 times smaller in magnitude (see Supplementary Figures S1 and S2).

Evolution of Relaxation-Activated Genes In our model, the expression of a gene that doesn't interact with its neighbors increases with the amount of negative supercoiling at its promoter (see Equations 3 and 4 in Methods). One could therefore expect that the genes of evolved individuals would present a qualitatively similar response. In order to verify this, we measured the expression of every gene in the genomes of evolved individuals, not only in the two discrete environments characterized by $\delta\sigma_A$ and $\delta\sigma_B$ (as throughout the evolutionary process), but instead as a function of a continuously varying $\delta\sigma_{env}$. Figure 4 presents this data, grouping genes by their type, and averaging over the 30 replicates.

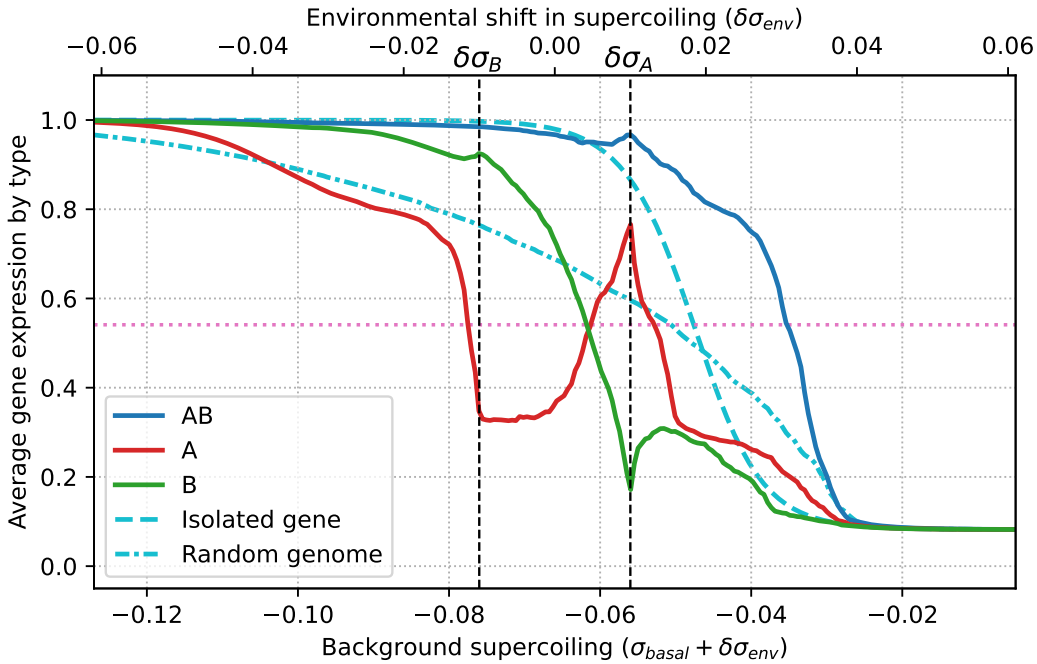

Figure 4: Average gene expression level per gene type as a function of the environmental perturbation in supercoiling. The full colored lines show average expression levels for each gene type (AB, A, and B in blue, red, and green respectively), as a function of the perturbation $\delta\sigma_{env}$ (top horizontal axis), or equivalently of the background supercoiling level $\sigma_{basal}+\delta\sigma_{env}$ (bottom horizontal axis), averaged over the best individual in each of the 30 populations. The dashed light blue line represents the expression level of a single neighbor-less gene, and the dash-dotted light blue line represents the average expression level of genes on 30 random genomes. The dashed vertical lines represent the perturbations $\delta\sigma_A$ and $\delta\sigma_B$ due to environments A and B, in which individuals evolved during the simulation, and the pink horizontal line marks $e_{1/2}$, the threshold above which a gene is considered active.

Figure 4 highlights striking differences between the average response of each type of gene in evolved genomes (red, green, and blue lines) on the one hand, and the responses of isolated, non-interacting genes (dashed light blue line) or of genes in random non-evolved genomes (dash-dotted light blue line) on the other hand. While AB and B genes (in blue and green respectively) display an average expression level that decreases as supercoiling increases, and that remains qualitatively similar to the behavior of random genes (dash-dotted line), A genes (in red) display a completely different behavior. Indeed, A genes show a non-monotonic response to the environmental perturbation in supercoiling, as their average expression level decreases until a local minimum in expression at $\delta\sigma_B$, then increases – even though background negative supercoiling decreases – until a local maximum at $\delta\sigma_A$, before decreasing again similarly to other genes types. In other words, due to their interaction with other genes, A genes present a phenotype of activation by environmental relaxation of DNA for perturbations

between $\delta\sigma_B$ and $\delta\sigma_A$, even though the activity of an isolated A gene would decrease with background DNA relaxation (dashed light blue line). The evolution of this relaxation-activated phenotype is furthermore very robust to the magnitude of the environmental perturbations, as we can again observe it when replaying the main experiment with supercoiling perturbations that are 10 or 100 times smaller than in the main experiment (see Supplementary Figures S3 and S4 respectively).

In our model, the transcription-supercoiling coupling is therefore able to provide a regulatory layer that mediates the transcriptional response to the global variation in DNA supercoiling due to environmental perturbations. Remarkably, the coupling allows for the evolution of activation by DNA relaxation, meaning that a global decrease in negative supercoiling can lead to a localized increase in negative supercoiling, and therefore demonstrating the importance of relative gene positions on the regulation of transcription.

2.2 Evolution of Local Genome Organization

Having first shown that differentiated gene transcription patterns can evolve in our simulations in response to environmental perturbations, we then sought to determine the genome organization that necessarily underlies these patterns in our model, given that the only difference between individuals in the model is the relative position and orientation of the genes on their genomes.

In order to do so, we systematically enumerated all possible pairs and triplets of neighboring genes of different types and in different relative orientations, and measured their abundances in evolved genomes, which we will describe starting with gene pairs. As the interaction in a gene pair can be asymmetric if the genes are in tandem, we gave gene pairs an orientation by considering that a pair consists of a focal gene which affects a target gene. We first measured the abundance of such oriented gene pairs in each relative orientation (convergent, divergent, focal gene upstream, or focal gene downstream), as the relative orientation of two neighboring genes determines their mode of interaction through the transcription-supercoiling coupling: mutual activation for divergent genes, mutual inhibition for convergent genes, and activation (resp. inhibition) of the upstream (resp. downstream) gene by the downstream (resp. upstream) gene. As, in our model, different gene types must evolve different activation patterns in each environment for an individual to have high fitness, we further stratified these pair counts by the type of each gene in the pair, resulting in 9 kinds of oriented pairs. Finally, in order to quantify the actual strength of the coupling between the genes in a given type of pair, we also measured the total level of positive and negative supercoiling generated by the transcription of the

focal gene at the promoter of the target gene, for all relative orientations. These data are presented in Figure 5.

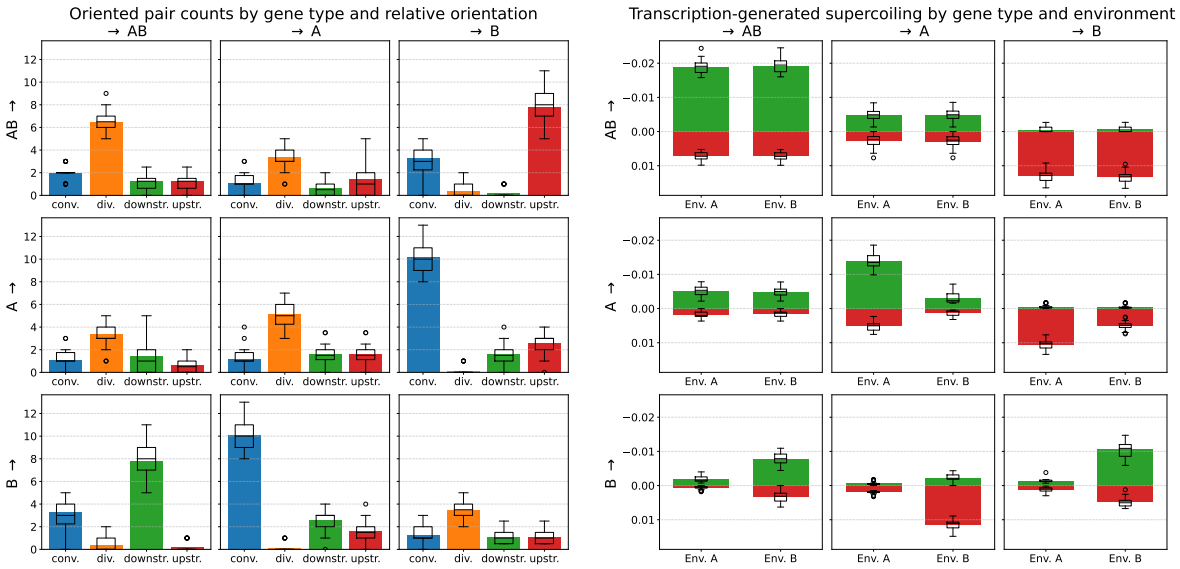

Figure 5: Interactions in oriented pairs of neighboring genes. The left-hand side panel shows the number of oriented pairs of each kind, split by the type of the focal gene (row) and of the target gene (column) in the pair, and by relative orientation (bars in each sub-panel: convergent, divergent, focal upstream, or focal downstream). For instance, the $AB \to B$ top-right panel shows the influence of AB genes on B genes, and the $B \to AB$ bottom-left panel the influence of B genes on AB genes (in the same pairs). In these pairs, there are on average 7.8 AB genes directly upstream of a B gene (top-right panel, in red), or equivalently 7.8 B genes directly downstream of an AB gene (bottom-left panel, in green) on an evolved genome. The right-hand side panel shows, for each kind of oriented pair, the total amount of negative (green) and positive (red) transcription-generated supercoiling due to the focal type (row) measured at the promoter of the target type (column), summed over all orientations, and split by environment. All data is averaged over the final best individual of each of the 30 replicates. Box plots indicate the median and dispersion between replicates, and circles denote outliers.

Frequent Gene Pairs in Evolved Genomes Showcase Twin-Domain Behaviors The most frequent pair pattern found in evolved genomes is that of a convergently oriented $\overrightarrow{A} - \overleftarrow{B}$ pair (or, equivalently, a $\overrightarrow{B} - \overleftarrow{A}$ pair, using overhead arrows to denote relative gene orientation). There are on average just over 10 such pairs in an evolved genome (blue bars in the $A \to B$ and $B \to A$ panels on the left-hand side of Figure 5). In such pairs, according to the twin-domain model of supercoiling, each gene theoretically inhibits the expression of the other gene in the pair through the downstream generation of positive supercoiling. The right-hand side panel of Figure 5 shows that, in environment A, A genes indeed generate an average positive supercoiling variation of 0.01 at the promoter of convergently oriented B genes, and hence decrease the expression of such B genes with a strength that is comparable to the supercoiling perturbation due to environment A ($\delta\sigma_A = 0.01$). In this

environment, B genes are mostly inhibited, and therefore do not strongly impact the expression of A genes. In environment B, it is oppositely B genes that strongly inhibit the expression of convergently oriented A genes, through the generation of positive supercoiling at the promoter of such A genes. In evolved genomes, convergent $\overrightarrow{A} - \overleftarrow{B}$ gene pairs therefore seem to behave as toggle switches, or bistable gene regulatory circuits, in which the expression of one gene represses the expression of the other gene (Gardner et al., 2000).

The second most frequent pattern is that of AB genes placed immediately upstream of a B gene, or $\overrightarrow{AB} - \overrightarrow{B}$ pairs, with on average just under 8 such pairs found in an evolved genome. This can be again understood in terms of the expression target of the genes in the pair: as visible in the right-hand side panel of Figure 5, AB genes in such pairs generate a large amount of positive supercoiling at the downstream B gene, which is needed for inhibition in environment A, and compensated by the negative supercoiling perturbation of environment B.

Finally, divergently oriented pairs of all three kinds of genes are also frequently found in evolved genomes. In particular, divergent $\overleftarrow{AB} - \overrightarrow{AB}$ gene pairs generate an average negative supercoiling of around -0.012 at their promoters, in both environments (summing the positive and negative bars in the $AB \rightarrow AB$ sub-panel on the right-hand side of Figure 5). This value is comparable in magnitude to, but has the opposite sign than, the supercoiling perturbation due to environment A ($\delta\sigma_A = 0.01$). The interaction between neighboring genes can therefore locally counteract the global shift in supercoiling caused by this environment, in order to maintain environment-agnostic high gene expression levels. This unconditionally positive feedback loop would, on the contrary, seem less evolutionarily favorable for $\overleftarrow{A} - \overrightarrow{A}$ or $\overleftarrow{B} - \overrightarrow{B}$ pairs than for $\overleftarrow{AB} - \overrightarrow{AB}$ pairs, as both A genes and B genes must be conditionally expressed or inhibited depending on the environment. We can indeed observe that divergent $\overleftarrow{A} - \overrightarrow{A}$ and $\overleftarrow{B} - \overrightarrow{B}$ pairs result in slightly weaker interactions (middle and bottom-right sub-panel of the right-hand side of Figure 5), in the environment in which these genes are active. In contrast to these frequent pairs, one can note that divergent $\overleftarrow{A} - \overrightarrow{B}$ gene pairs are almost never found, consistently with theoretical expectation, since A and B genes must not be expressed in the same environment.

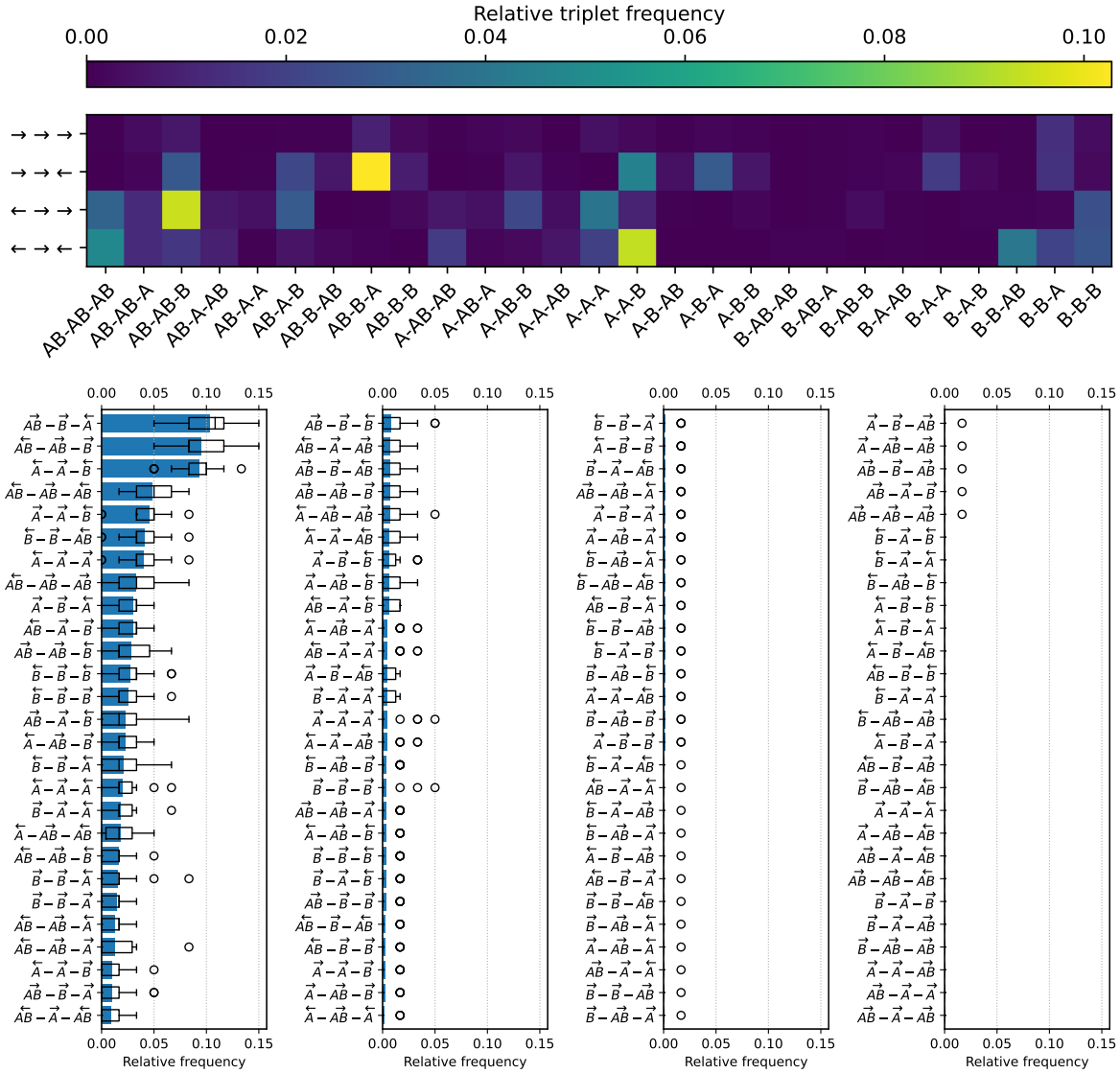

Figure 6: Relative frequencies of gene triplets. Top: heatmap of relative gene triplet frequencies, with gene types on the X-axis and relative gene orientations on the Y-axis. Note that we count symmetric triplets together, keeping by convention the triplet whose central gene is in leading orientation. Bottom: gene triplets sorted by decreasing relative frequency (top to bottom and left to right), with relative gene orientations depicted as overhead arrows. All data is averaged over the best final individuals of the 30 replicates. Box plots indicate the median and dispersion between replicates, and circles denote outliers.

Gene Triplet Frequencies Reflect Pairwise Interactions Following the same approach as for pairs, we then measured the observed frequencies of gene triplets, stratifying triplets by the type and orientation of each gene they contain, which results in $3^3 * 2^3 = 216$ possible triplets. We grouped symmetric triplets together (for example, $\overrightarrow{AB} - \overrightarrow{B} - \overleftarrow{A}$ together with $\overrightarrow{A} - \overleftarrow{B} - \overleftarrow{AB}$), keeping by

convention triplets whose central gene is in leading orientation, thus reducing the number of triplets under consideration to 108.

Figure 6 shows the gene triplet frequencies observed in the genomes of the best individuals at the end of the simulations, sorted by gene type and orientation (top heatmap) or by decreasing frequency (bottom bar and box plots). As in the case of pairs, triplet frequencies strongly depend on their gene content: in particular, three specific triplets stand out as much more frequent than all others. These triplets are visible as yellow-green squares in the heatmap at the top of Figure 6: by decreasing frequency, $\overrightarrow{AB} - \overrightarrow{B} - \overleftarrow{A}$ (1), $\overleftarrow{AB} - \overrightarrow{AB} - \overrightarrow{B}$ (2), and $\overleftarrow{A} - \overrightarrow{A} - \overleftarrow{B}$ (3). The fact that these are the most frequent triplets is consistent with the previously discussed distribution of frequent gene pairs, as each of these triplets contains either a divergent $\overleftarrow{AB} - \overrightarrow{AB}$ pair or a convergent $\overrightarrow{A} - \overleftarrow{B}$ pair, and allow us to gain further insight about the regulation of these pairs. Indeed, triplet (1) shows how the B gene of a convergent $\overrightarrow{A} - \overleftarrow{B}$ pair can be under inhibitory control of an AB gene (remember that, with a bacteria-like negative level of basal supercoiling, it is harder to inhibit than to activate gene expression). Triplet (2) shows how an AB gene in a strongly-expressed divergent $\overleftarrow{AB} - \overrightarrow{AB}$ pair can inhibit a B gene, and the B gene of the triplet can also be seen as reinforcing the expression of the divergent $\overleftarrow{AB} - \overrightarrow{AB}$ pair in environment B. Finally, triplet (3) shows how the A gene of a convergent $\overrightarrow{A} - \overleftarrow{B}$ pair can be activated by a divergent A gene, and shows a possible synergy between overlapping divergent $\overleftarrow{A} - \overrightarrow{A}$ and convergent $\overrightarrow{A} - \overleftarrow{B}$ gene pairs. Similarly to gene pairs, it is noteworthy that 22 out of 108 possible triplets never appear at all in evolved genomes (rightmost subplot of Figure 6), and an additional 17 triplets appear only once, suggesting that those triplets are under strong negative selection.

In the model, specific local genome organization patterns can therefore be evolutionarily selected or counter-selected in order to attain favorable gene expression levels through supercoiling-mediated interactions. In particular, we observed the formation of divergent gene pairs or convergent toggle switches, that either regulate or are under the regulation of their neighboring genes. However, there is no reason why phenotypically important interactions should be limited to pairs or triplets of genes, as there are always more neighboring genes just outside a given pair or triplet. As a systematic exploration would become combinatorially intractable and statistically meaningless for wider gene neighborhoods, we then studied how the behavior of a given gene depends on its neighbors at all distances.

2.3 Gene Inhibition Requires Medium-Range Interactions

As we just saw, the local organization of the genome seems to play an important role in the regulatory response to environmental changes in supercoiling in the model. However, this local response cannot suffice to completely explain the environment- and gene-type- specific activation patterns that we observed above. Indeed, in the dense bacteria-like genomes of individuals in our model, genes do not only interact through supercoiling with their closest neighbors, but also with genes located further away on the genome. In order to quantify more precisely the range at which regulatory interactions take place in evolved genomes, we therefore studied how gene expression changes when isolating genes into contiguous neighborhoods of increasing sizes.

We applied the following algorithm: for every gene on a given genome, and for every odd subnetwork size k between 1 and the genome size, we extracted the subnetwork of k consecutive genes centered around that gene. Then, for each such subnetwork, we computed the expression level of every gene in the subnetwork (in the same way as for a complete genome) in each environment, and compared the activation state of the central gene with its state in the complete genome. This allowed us to compute the following metric: the minimum subnetwork size at which a gene presents the same activation state (that is, activated or inhibited) as in the complete genome, in each environment. We interpret this metric as an indicator of the complexity of the interaction network required to produce the behavior of that particular gene in that environment. Two representative examples of this algorithm are presented in Figure 7, and complete data are then shown in Figure 8.

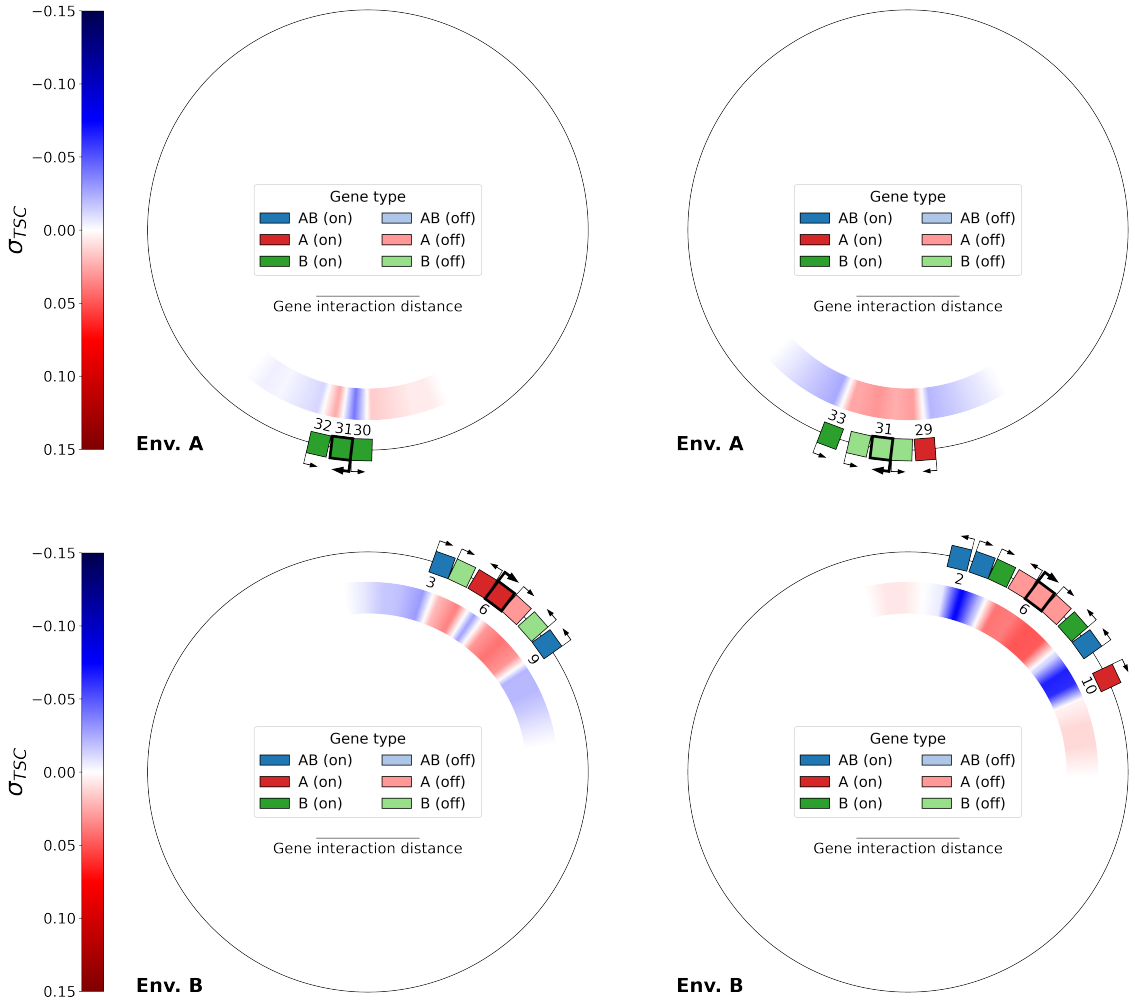

Figure 7: Top: contiguous subnetworks of size 3 (left) and 5 (right) centered around gene 31 (of type B, in bold) of the final best individual of replicate 21, evaluated in environment A. Bottom: contiguous subnetworks of size 7 (left) and 9 (right), centered around gene 6 (of type A, in bold) of the same individual, evaluated in environment B. In each case, when moving from the smaller to the larger subnetwork, the activation state of the central gene switches from activation to inhibition, which is the original state of these genes in the complete genome of this individual (shown in Figure 1).

Figure 7 depicts the smallest subnetworks that are required in order to obtain the inhibition of a representative gene of type B in environment A (top row, gene 31), and of a representative gene of type A in environment B (bottom row, gene 6), both taken from the genome of the same evolved individual as in Figure 1. The central B gene in this example is not inhibited by a subnetwork of size 3, but requires a subnetwork of size 5 in order to be inhibited, and, similarly, the central A gene is not inhibited by a subnetwork of size 7, but requires a subnetwork of size 9 in order to be inhibited.

In each case, increasing the size of the subnetwork by two (one gene on each side) drastically changes the expression level of the central gene, alongside with the associated level of transcription-generated supercoiling. Indeed, in the two subnetworks centered around the B gene (top), all 3 genes in the small subnetwork switch from activation in the small subnetwork to inhibition in the large subnetwork, and in the two subnetworks centered around the A gene (bottom), the two B genes and two out of the three central A genes also switch from activation to inhibition when moving from the small to the large subnetwork. In both examples, the activity of a gene does therefore not only depend only on its interaction with its closest neighbors, but with a broader section of the genome.

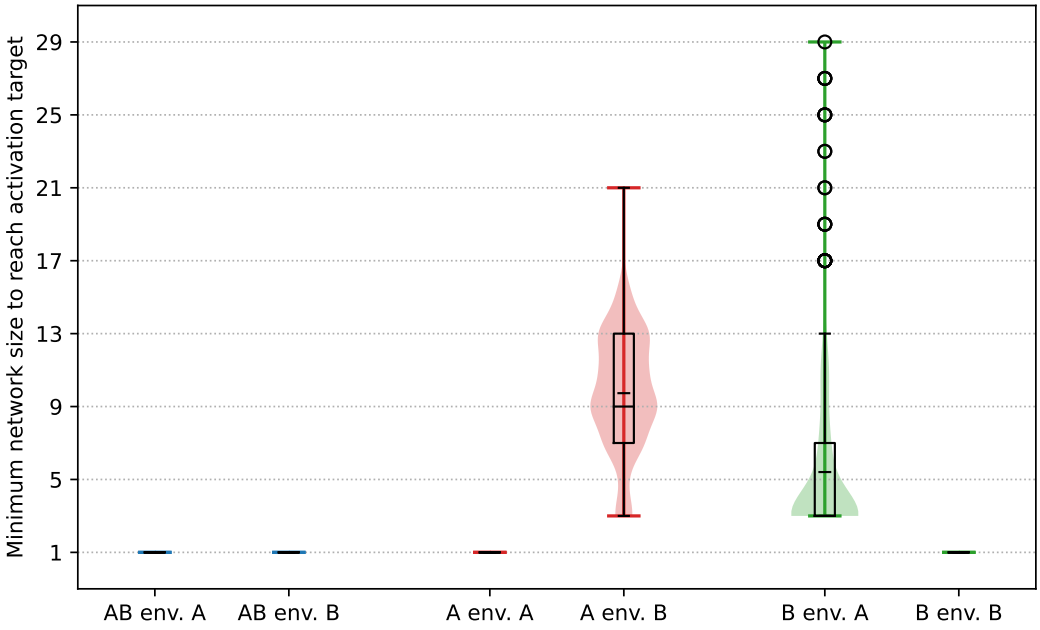

Figure 8: Minimal contiguous subnetwork size required for the central gene in the subnetwork to present the same activation state as in the complete genome, for each gene type, and in each environment. The data is computed only for genes in the best final individual of each replicate which present the correct activation state in both environments (97.7% of AB genes, 92.7% of B genes and 53.2% of A genes). In each case, a box plot is overlaid on a violin plot representing the whole distribution, the mean is represented by the smaller tick in the box plot, and circles denote outliers.

We then computed these minimal subnetwork sizes for every gene that presents the correct activation state in each environment in the final best individual of each of the 30 replicates. Markedly different patterns again appear, depending on whether the targeted behavior for the gene is activation or inhibition, as depicted in Figure 8. For AB genes in both environments, as well as for A genes in environment A and B genes in environment B, the experimentally obtained minimum subnetwork size is 1, consistently with the supercoiling response of an isolated gene (previously shown in Figure 4). In-

deed, with a basal supercoiling value of $\sigma_{basal} = -0.06$, an isolated gene experiences a high expression level in both environments – even without interactions – in the model, as in real-world bacteria.

When the expression target of the gene is inhibition, that is for A genes in environment B and for B genes in environment A, the picture is however quite different. In this case, a significantly larger subnetwork is required in order to obtain inhibition of the focal gene: The median subnetwork size required to inhibit A genes in environment B is 9, or 4 genes on each side. For B genes, the median subnetwork size for inhibition in environment A is lower than that required for the inhibition of A genes in environment B, but higher than when the target is activation: Genes always need at least a subnetwork of size 3 (1 gene on each side), and several outliers need a subnetwork of more than 20 genes in order to obtain inhibition.

The gene interaction networks that evolve through the transcription-supercoiling coupling therefore exhibit a structure that cannot be explained only by local interactions, but that can on the contrary require the participation of a significant number of genes in order to allow genes to reach their required environment-specific expression levels.

2.4 A Whole-Genome Gene Interaction Network

Having shown that the transcription-supercoiling coupling plays a major role in the regulation of gene expression in our model, and that supercoiling-mediated interactions can implicate more than just neighboring genes, we then sought to describe these interactions in more detail by viewing the genome as a network of interacting genes. The matrix of gene interactions used to compute gene expression levels, whose coefficients $\frac{\partial \sigma_i}{\partial e_j}$ represent the effect of the transcription of every gene on the local level of supercoiling at every other gene (and decrease linearly with distance, see Equation 1 in Methods), could seem to provide a natural graph representation of the interactions between the genes in the genome of an individual. However, as this matrix does not take into account actual gene expression levels, using it directly could provide an inaccurate picture of the effective interactions between genes (for example, overestimating the influence of a weakly-expressed gene). We therefore constructed an *effective* interaction graph, by measuring instead the effect of gene knockouts on gene expression levels.

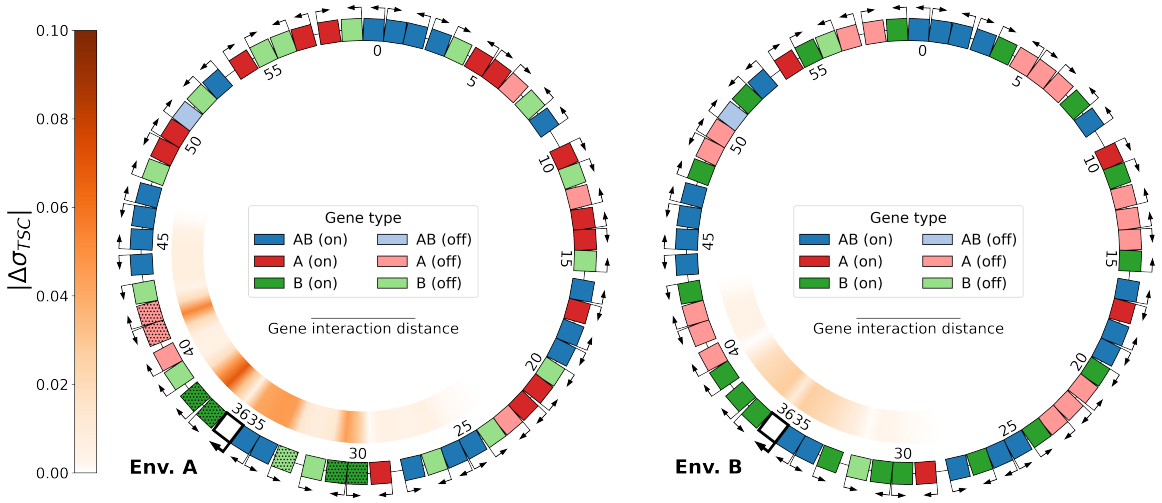

Figure 9: Knockout of gene 36 (of type *AB*, in bold, colored white) of the final best individual of replicate 21, evaluated in environments A (left) and B (right). Hatched genes represent genes whose activation state is switched by the knockout when compared to the original genome. The inner ring represents the absolute difference $|\Delta\sigma_{TSC}|$ in the level of transcription-generated supercoiling between the knockout genome and the original genome (shown above in Figure 1).

Gene Knockouts Gene knockout is a genetic technique in which a gene of interest is inactivated (knocked-out) in order to study its function (in our case, its possible role as part of a gene interaction network). In order to knock out a given gene in an individual in our model, we set the transcription rate of that gene to zero during the computation of gene expression levels (as described in Methods). This mimics a loss of function of the promoter of the gene, while keeping the intergenic distance between its upstream and downstream neighbors unchanged, thereby minimizing differences to the original individual. The result of a gene knockout on the genome of an evolved individual is shown in Figure 9. The knocked-out gene is gene 36 (bottom left of the genome), which is of type *AB* and originally activated in both environments (see Figure 1 for the original genome of the same individual). We can see that, in environment A, knocking out this gene results in a switch in the activation state of 7 genes (hatched in the left-hand side of Figure 9), and that these genes are not all contiguously located. This knockout also results in local supercoiling changes that propagate up to the bottom-left third of the genome, outside of the direct influence of the knocked-out gene. In environment B, knocking out this gene instead results in milder supercoiling changes that do not result in any gene switching state. In this example, knocking out even a single gene can therefore substantially affect gene expression levels, and lead to a switch in the activation state of other genes on the genome, even when these genes do

not directly interact with the knocked-out gene.

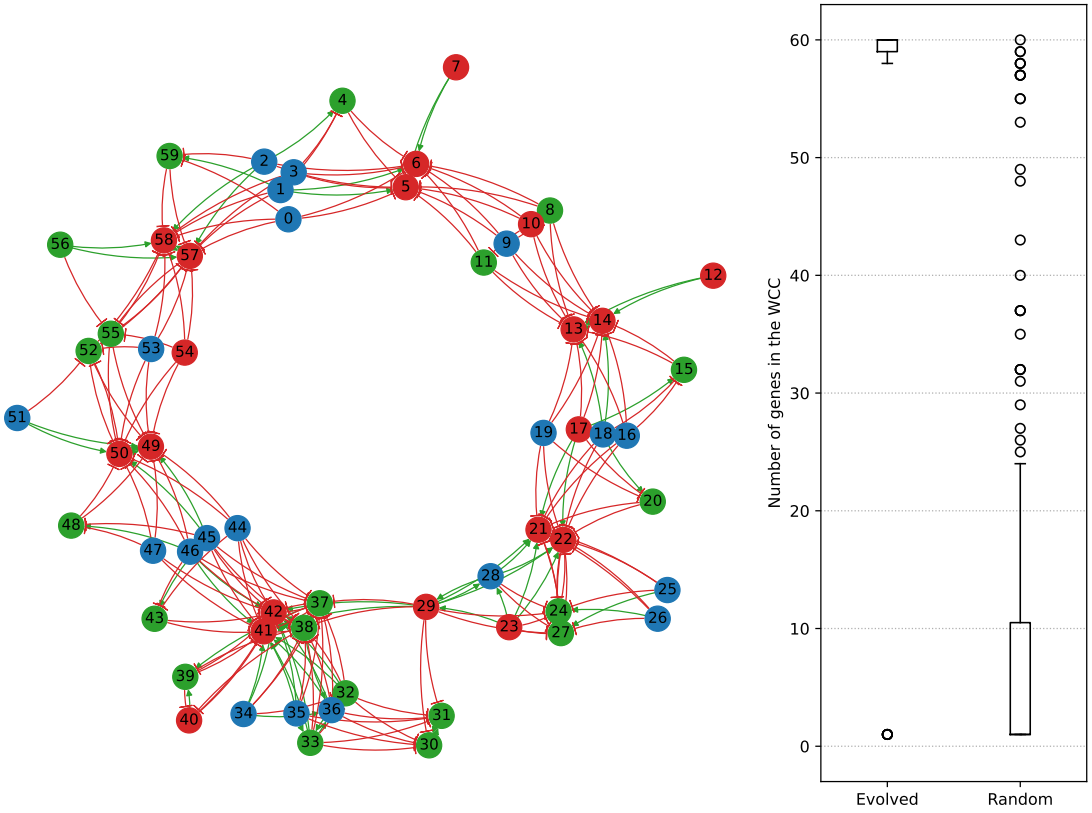

Figure 10: Left: effective interaction graph of the best individual at the last generation of replicate 21, obtained by knocking out every gene one by one and measuring the resulting gene switches in either environment. Activation edges are drawn in green, and inhibition edges in red. Gene numbering is the same as in Figures 1, 8 and 9. Right: box plot representing the distribution of weakly connected component (WCC) sizes in the effective interaction graphs of evolved individuals (left) compared to random individuals (right). Circles outside the box plot whiskers denote outliers.

Constructing the Effective Interaction Graph We construct the effecting interaction graph in the following manner: we successively knock out every gene in the genome, and each time add edges from the knocked-out gene to every other gene whose activation state is switched by the knockout in either environment. If the knockout switches off a gene that was originally activated in the complete genome, we mark the edge as an activation edge, meaning that the knocked-out gene was necessary in order to activate the switched-off gene. If the knockout conversely switches on a gene that was originally inhibited in the complete genome, we mark the edge as an inhibition edge. If knocking out a gene switches on or off the same other gene in the two environments, we only add a single edge (even if one edge is an activation edge and the other an inhibition edge), as our main focus is on the

connectedness of the resulting graph. The effective interaction graph of the example evolved individual in Figure 9 is presented on the left-hand side of Figure 10. In this individual, there is only one weakly connected component (WCC), meaning that all the genes of this individual contribute to a single, whole-genome interaction network.

Global Structure of the Effective Interaction Graphs In order to characterize the effective interaction graphs of evolved individuals, we compared them with the effective interaction graphs of 30 random individuals drawn using the same genome parameters (shown in Table 1 in Methods) as the initial individuals used at the beginning of evolution. The distribution of WCC sizes for each group of graphs are presented on the right-hand side of Figure 10. As we can see, the effective interaction graphs of evolved individuals are clearly different from those of random individuals. Indeed, evolved genomes have WCC sizes of 58 to 60 genes (left), comprising every or nearly every gene on the genome, along with very few single-gene WCCs. In particular, in 26 out of the 30 evolved populations, the interaction graph of the best individual comprises only a single WCC that includes every gene on the genome, similarly to the interaction graph in Figure 10. In random genomes (right), on the contrary, WCC sizes span the whole range from single-gene to whole-genome WCCs, with most of the connected components counting less than 10 genes.

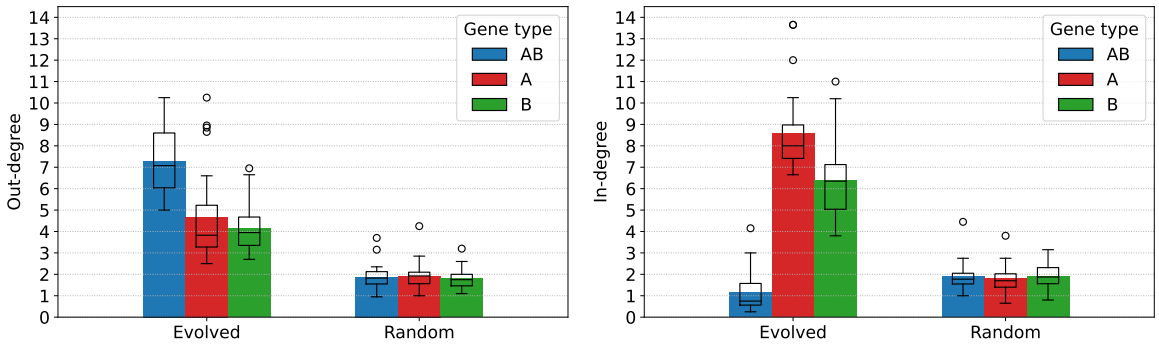

Figure 11: Left: average out-degree (number of genes switched by knocking out a given gene) of the nodes in the effective interaction graph, separated by gene type, for evolved and random individuals. Right: average in-degree (number of genes whose knockout switches a given gene) of the nodes in the effective interaction graph, separated by gene type, for evolved and random individuals. Box plots show the median and dispersion around the average value, and circles represent outliers.

Local Structure of the Effective Interaction Graphs Evolved genomes are indeed on average much more connected than random genomes, as we can see in Figure 11, which presents the out- and in-degree of genes (averaged by gene type) in the effective interaction graphs. The left-hand side of

Figure 11 first shows the average out-degree of each gene type (i.e., the number of genes that are switched either on or off by knocking out a gene of that type). While knocking out a gene in a random genome switches the state of a little less than 2 other genes on average, independently of the type of the knocked-out gene, this number is much higher in evolved genomes. Knocking out A or B genes switches 4 other genes on average, and knocking out AB genes switches up to 7 other genes. Through this higher connectedness, AB genes therefore play a quantitatively more important regulatory role than A genes or B genes. This can be explained by the fact that AB genes are activated – and generate more supercoiling through transcription, as shown in Figure 5 – in both environments, while most A and B genes are instead inhibited in one environment or the other.

When looking at the in-degree of genes (the number of genes whose knockout will switch a given gene on or off) on the right hand-side of Figure 11, we can see that evolved genomes are again much more connected on average than random genomes, and that the in-degree of genes greatly depends on their type. Indeed, AB genes are only switched by one other gene on average, meaning that their activation state is robust to perturbations in the interaction network. The robustness of AB genes could be expected, as these genes must have the same activation state in both environments in order to attain high fitness. A genes and B genes have an oppositely much higher in-degree, meaning that their activation state relies on the regulatory action of a large number of other genes. Similarly to AB genes, this high connectedness could be expected, as a high in-degree could make A and B genes more sensitive to variations between the two environments.

In our model, the evolution of relative gene positions on the genome therefore integrates local supercoiling-mediated interactions between neighboring genes into a single genome-wide interaction network, through which all genes interact in order to reach their targeted expression levels.

3 Discussion and Perspectives

DNA supercoiling, through its effect on promoter activation and hence on gene transcription (Dorman and Dorman, 2016), is an important actor of the regulatory response of bacteria to diverse environmental conditions (Martis B. et al., 2019). But gene transcription itself has long been posited to impact the level of DNA supercoiling in return, as suggested by the twin-domain model of supercoiling (Liu and Wang, 1987), and it has since been shown to indeed play a major role in shaping the bacterial DNA supercoiling landscape (Visser et al., 2022), through what has been termed the transcription-supercoiling coupling (Pruss and Drlica, 1989; Meyer and Beslon, 2014). Taken together, these results

suggest that such supercoiling-mediated interactions between the transcription rates of neighboring genes could play a part in regulating bacterial gene activity, and might hence influence the evolution of bacterial genome organization.

In this work, we therefore sought to assess the possibility of the evolution of such supercoiling-based gene regulation in an *in silico* bacteria-like model, and to determine its potential hallmarks on the local and global organization of bacterial genomes. To this end, we developed an evolutionary model of the transcription-supercoiling coupling, in which populations of individuals must evolve differentiated gene expression levels in response to two different environmental conditions. We showed that, in this model, gene regulation by DNA supercoiling is indeed a sufficient mechanism to evolve environment- and gene- specific patterns of activation and inhibition. In particular, we observed the emergence of relaxation-activated genes that respond to supercoiling oppositely to the majority of genes, which are classically inhibited by DNA relaxation (Forquet et al., 2021). Our results therefore demonstrate that, in theory, this response to supercoiling can result not only from promoter sequence – as in the case of the *gyrA* promoter (Menzel and Gellert, 1987) – or spacer length (Forquet et al., 2022), but also from local genome organization, as already proposed by Sobetzko (2016) or El Houdaigui et al. (2019). As such, these findings suggest that supercoiling-mediated regulation could be a sufficient mechanism to adapt gene expression in response to environmental constraints. This regulatory role could in particular be especially important in bacteria that lack other regulatory mechanisms, such as the genome-reduced *B. aphidicola* (Brinza et al., 2013) or *M. pneumoniae* (Yus et al., 2019).

We then investigated the patterns of genome organization that underlie this transcriptional response to different supercoiling environments in the model. At the most local scale, we found that evolved genomes are enriched in divergent pairs of always-on genes that form positive feedback loops, as well as in convergent pairs that oppositely act as bistable toggle switches controlled by supercoiling rather than by transcription factors (Gardner et al., 2000). The existence of such supercoiling-mediated toggle switches had been earlier posited by using mechanistic biophysical models that explicitly describe the movement of RNA polymerases during gene transcription (Sevier and Hormoz, 2022; Johnstone and Galloway, 2022), and their emergence in our model suggests that such toggle switches could indeed evolve as a means to regulate the expression of neighboring genes (note that other models, such as Kim et al. (2019), suggest that divergently transcribing polymerases could slow down transcription, complexifying the interaction between neighboring genes). We additionally found that, similarly to pairs, the distribution of gene triplets in evolved genomes is not uniform, but is enriched in configurations

that are theoretically predicted to be beneficial in the model. Then, we showed that such interactions between pairs or triplets are in fact not entirely sufficient to selectively activate or inhibit genes in specific environments, but that interactions between larger groups of genes can be required to do so. Such regulation of gene expression through the interaction of groups of co-located genes could help explain the persistence of synteny segments (clusters of genes that display correlated transcription levels at the supra-operonic scale) that has been evidenced in bacterial evolutionary histories (Junier and Rivoire, 2016). Indeed, if local interactions play a role in regulating the expression of groups of neighboring genes, genomic rearrangements that alter relative gene positions within these structures could disrupt their regulation and hence be evolutionarily unfavorable. Finally, we characterized in further detail the gene interaction networks that evolve in the model by adapting the classical genetics tool of gene knockouts (Baba et al., 2006). We showed that supercoiling-mediated interactions integrate the entire genome of evolved individuals into a single connected network of interacting genes, in opposition to the sparse, disconnected networks displayed by randomly generated individuals. Moreover, we showed that genes play different roles in these networks depending on their type, corresponding to the type-specific responses to environmental variations that genes must display in the model. Overall, our simulations therefore demonstrate that, in this model, the transcription-supercoiling coupling provides a strong and precise regulatory mechanism that allows for the evolution of complex regulation patterns based solely on the relative positions of genes on the genome, and that this regulation can be sensitive to even very small environmental perturbations (see Supplementary Material). Our simulations furthermore provide insight on the possible impact of this particular mode of regulation on the structure of bacterial genomes, both at the local and global scales.

In this work, we voluntarily kept our model as simple as possible in order to obtain easily interpretable results, while retaining the core concept of the transcription-supercoiling coupling. In particular, in order to keep simulations computationally tractable, we restricted the number of genes in each individual to 60, much fewer than the around 4,300 genes in the *E. coli* genome (Blattner, 1997), but importantly keeping chromosome size much larger than the supercoiling interaction distance, so that each gene directly interacts with a small proportion of the genome only. Increasing the number of genes in our model should in principle therefore not affect the local- and medium-scale patterns that we observe, nor the formation of large-scale interaction networks, although such genomes might harbor several large weakly connected components rather than a single one.

By modifying the model appropriately, an number of adjacent relevant questions could also be

studied. We chose to use a deterministic algorithm to compute the gene expression levels resulting from the transcription-supercoiling coupling for a given value of $\delta\sigma_{env}$. Stochastic approaches could be considered, for example averaging final expression levels over slightly perturbed initial gene expression levels. We do not expect such model changes to qualitatively affect the results, but they could provide additional information about the stability of the evolved gene regulatory networks. Increasing the number of environments that individuals face, and accordingly increasing the number of gene types, might provide a larger panel of evolutionarily selected local gene organizations that might reflect more accurately the real-world diversity of bacterial genomes. In another direction, it would also be interesting to study how including transcriptional read-through, or the transcription of successive genes by a single RNA polymerase, would alter the genomic structures that evolve in our model. Indeed, this mechanism has also been hypothesized to play a part in the evolutionary conservation of synteny segments in bacterial genomes, by correlating the expression levels of genes in these segments (Junier and Rivoire, 2016). Similarly, letting the response to supercoiling of gene promoters coevolve with genomic organization could help understand the evolution of unusual promoters such as the *gyrA* promoter, which is activated by relaxation due to its particular sequence (Menzel and Gellert, 1987). Finally, integrating a classical model of gene regulation via transcription factors to our model, such as the one presented by Crombach and Hogeweg (2008), could also help shed light on the coevolution between the different modes of gene regulation that are available to bacterial genomes. From a theoretical standpoint, a range of mechanistic biophysical models of the transcription-supercoiling coupling have been put forward, using different hypotheses in order to address related questions on this topic. Brackley et al. (2016) show a phase transition in the transcription regime as the number of RNA polymerases transcribing a given gene increases; Sevier and Hormoz (2022) show that bursty transcription can emerge from the transcription-supercoiling coupling; and Meyer and Beslon (2014) and El Houdaigui et al. (2019) try to predict gene expression levels quantitatively, as a function of the local level of DNA supercoiling. An important validation of these complementary approaches would therefore be to investigate the extent to which these models, including ours, conform to one another as the level of abstraction changes. From an experimental standpoint, comparing the simulated frequencies of genes in given pair or triplet relative organizations that we observe, as well as the correlation of the expression levels for genes involved in such patterns, with data from real-world bacteria could also help determine the extent of the regulatory role of supercoiling in these organisms. In particular, an experimental validation of the model could be obtained by quantifying the correlation between

genomic organization and gene transcription levels in species with few transcription factors such as *B. aphidicola* (Brinza et al., 2013). This could be done by reusing the analyses applied to *E. coli* and *S. pneumoniae* in Sobetzko (2016). Finally, from a synthetic biology point of view, a better understanding of the regulatory interactions that result from the transcription-supercoiling coupling could help design more finely controlled artificial genetic constructs, as is being explored in Johnstone and Galloway (2022) or Boulas et al. (2023).

4 Conclusion

To the best of our knowledge, this work is the first to propose a model to investigate the role of the coupling between gene transcription and DNA supercoiling in the evolution of the structure of bacterial genomes. By integrating a biophysical model of the transcription-supercoiling coupling into an evolutionary simulation, we have demonstrated the theoretical possibility of the evolution of gene regulation through a supercoiling-mediated regulatory network that allows for precise responses to variations in the environment. For experimentalists, this work provides a theoretical model that could help explain the heterogeneous transcriptomic response (with both up- and down-regulation of multiple genes) observed in bacteria confronted to supercoiling variations, due for example to virulence-inducing environments (Dorman, 2019) or to gyrase-inhibiting antibiotics (de la Campa et al., 2017). For evolutionists, it contributes to the hypothesis that the observed conservation of local gene order along bacterial evolutionary histories could be due to supercoiling-based regulation (Junier and Rivoire, 2016). Finally, for synthetic biologists, it provides a theory that could help predict more accurately the transcription levels that can be expected to result from a given gene context (Boulas et al., 2023), and could thus help in the design of new artificial genetic circuits.

5 Methods

This section details the model that we use throughout the manuscript to study the role of the transcription-supercoiling coupling in the evolution of gene regulation and genome organization in bacteria-like organisms. The model consists in an individual-based evolutionary simulation, in which individual whose phenotypes are computed according to a biophysical model of the effect of supercoiling on gene expression must adapt to two environments presenting different supercoiling levels. It is based upon and refines our previous model presented in Grohens et al. (2022). We start by presenting

the individual-level biophysical model, and describe how we compute gene expression levels based on their relative positions on the genome by taking into account the transcription-supercoiling coupling. Then, we describe how we compute the fitness of individuals by evaluating their adaptation to the two environments, and describe how we create new individuals and populations with genomic inversions. Finally, we present the experimental setup that we used in order to run the simulations presented in the Results section, and discuss code and data availability.

5.1 Individual-Level Model of the Transcription-Supercoiling Coupling

We define the genotype of an individual as a single circular chromosome, meant to represent a bacterial chromosome. The chromosome consists in a fixed number of protein-coding genes, which are separated by non-coding intergenic segments of varying sizes, and is additionally characterized by a basal supercoiling level σ_{basal}. Each gene on the chromosome is characterized by its starting position (note that genes cannot overlap in our model), its orientation (on the forward or reverse strand), its length, and its basal expression level. We always consider individuals within an environment, which we define by the perturbation $\delta\sigma_{env}$ that it imposes to the background supercoiling level of the chromosome. We define the phenotype of an individual in a given environment as the vector that holds the expression levels of all of its genes. We compute this phenotype by solving the system of equations given by the interaction of the individual's genes with one another through the transcription-supercoiling coupling (described below), on a chromosome with a background supercoiling level of $\sigma_{basal} + \delta\sigma_{env}$. Note that, while we do not have a formal proof that this system always has a single solution, this is empirically the case in the parameter range used in the simulations.

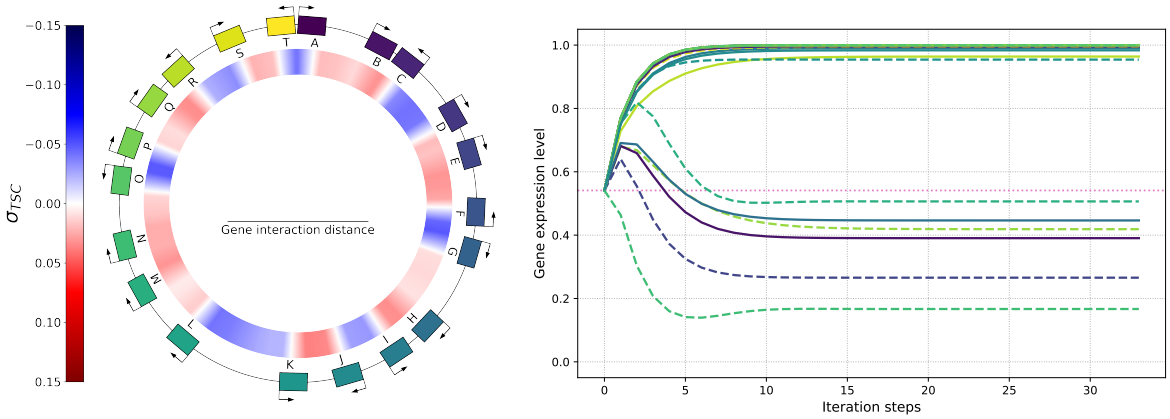

Figure 12: Left: genome (outer ring) and level of transcription-generated supercoiling (σ_{TSC}, inner ring) of an example individual with 20 genes placed at random positions and orientations and colored by position, with a gene length and average intergenic distance of 1 kb each, and a basal supercoiling level of $\sigma_{basal} = -0.066$. The individual is evaluated in an environment in which $\delta\sigma_{env} = 0$. Right: evolution of the expression level of each gene of the individual (reusing gene colors from the genome) during the computation of the solution to the system given by equations 2, 3, and 4, starting from initial expression levels of $e_{1/2}$. Solid lines represent genes on the forward strand, dashed lines genes on the reverse strand, and the dotted pink line represents $e_{1/2}$, the gene activation threshold.

The genome of an example individual with 20 genes is shown on the outer ring of the left-hand side panel of Figure 12. The inner ring depicts the local level along the genome of DNA supercoiling resulting from gene transcription, when this individual is evaluated in an environment with a supercoiling shift of $\delta\sigma_{env} = 0$. As expected from the twin-domain model of supercoiling, we can observe a buildup in negative supercoiling (in blue) between pairs of genes in divergent orientations, such as the C-D or F-G gene pairs, and a buildup in positive supercoiling (in red) between pairs of genes in convergent orientations, such as the K-J or Q-R gene pairs. The right-hand side panel of Figure 12 shows the computation of the gene expression levels for this individual in the same environment (as detailed below). Note that, in this model and throughout the manuscript, we conflate gene transcription rates with mRNA concentrations, as we assume that mRNAs are degraded at a constant rate, and as transcription rates in our model are only affected by the effect of supercoiling on transcription. We additionally conflate transcription rates with expression levels (or protein concentrations), as we again assume proteins to be translated at a rate proportional to the associated mRNA concentrations and degraded at a constant rate.

Effect of Transcription on Supercoiling For an individual with a genome containing n genes, we model the influence of the transcription of each gene on the level of supercoiling at the promoter of every other gene in the form of an n-by-n matrix, which we call the interaction matrix. The coefficient $\frac{\partial \sigma_i}{\partial e_j}$ at indices (i, j) in this matrix represents the infinitesimal variation in DNA supercoiling at the promoter of gene i due to the transcription of gene j. The value of this coefficient is given by Equation 1:

$$\frac{\partial \sigma_i}{\partial e_j} = \eta \cdot c \cdot \max(1 - \frac{d(i,j)}{d_{max}}, 0) \tag{1}$$

η gives the sign of the interaction, which depends on the position and orientation of gene j relative to gene i, according to the twin-domain model (Liu and Wang, 1987). If gene j is upstream of gene i, and if it is on the same strand as (points towards) gene i, then its transcription generates a buildup in positive supercoiling at gene i ($\eta = 1$). Conversely, if gene j is upstream of gene i but on the other strand than (points away from) gene i, it generates a buildup in negative supercoiling at gene i ($\eta = -1$). If gene j is instead located downstream of gene i, the sign of the interaction in each case is reversed: $\eta = -1$ if the genes are on the same strand, and $\eta = 1$ otherwise.

We then apply a torsional drag coefficient c, which is a high-level representation of the magnitude of the effect of transcription on the local supercoiling level. Finally, we model this change in supercoiling as linearly decreasing with the distance $d(i, j)$ between genes i and j. More precisely, we consider the distance between the promoter of gene i, the position at which the local level of supercoiling affects the probability that an RNA polymerase binds to the DNA and starts transcribing gene i, and the middle of gene j, the average location of the RNA polymerases that transcribe gene j, assuming that DNA is transcribed at a constant speed. When this distance reaches a threshold of d_{max}, we consider the two genes to lie too far away to interact, and the effect vanishes. In other words, d_{max} represents the maximum gene interaction distance on either side of a gene (see Figure 12). Finally, we consider that genes do not interact with themselves through supercoiling, so we set $\frac{\partial \sigma_i}{\partial e_i}$ to 0 for all i.

Effect of Supercoiling on Transcription In order to describe the effect of supercoiling on transcription, we adapted the equations and parameter values presented in El Houdaigui et al. (2019), which are based on the *in vitro* analysis of the transcription of model bacterial promoters. We first compute the local level of supercoiling σ_i at the promoter of gene i, which is the sum of the background supercoiling level $\sigma_{basal} + \delta\sigma_{env}$ (which is constant along the genome for any given individual in a given

environment), and of the local variation in supercoiling caused by the transcription of every other gene (represented in Figure 12 as σ_{TSC}):

$$\sigma_i = \sigma_{basal} + \delta\sigma_{env} + \sum_{j=1}^{n} \frac{\partial \sigma_i}{\partial e_j} e_j \tag{2}$$

We then compute the expression level of the gene using a thermodynamic model of transcription, in which transcription is approximated by a sigmoid that increases with negative supercoiling until a saturation threshold is reached (Forquet et al., 2021). More precisely, we compute the opening free energy U_i of the promoter of gene i, which depends on σ_i, the level of supercoiling at the promoter and on σ_0, the level of supercoiling at which the opening free energy is at half its maximum level, according to the following sigmoidal function:

$$U_i = \frac{1}{1 + e^{(\sigma_i - \sigma_0)/\varepsilon}} \tag{3}$$

We can then compute the expression level e_i of gene i, using an inverse effective thermal energy m:

$$e_i = e^{m(U_i - 1)} \tag{4}$$

The transcription level of a gene is therefore expressed in arbitrary units between e^{-m}, the minimum expression level when the promoter is most hindered by supercoiling (when $U_i = 0$), and 1, the maximum expression level, when the promoter is most activated by supercoiling (when $U_i = 1$). Throughout the manuscript, we describe a gene as activated if its transcription level is above the mean of these two values $e_{1/2} = \frac{1}{2}(e^{-m} + 1)$, and inhibited otherwise.

Computation of Gene Expression Levels Recall that we define the phenotype of an individual in an environment (described by $\delta\sigma_{env}$) as the vector of gene expression levels that is solution to the system of equations given by Equations 2, 3 and 4, in that environment. In order to compute this phenotype, we numerically compute a solution to the system of equations by using an iterative fixed-point algorithm, starting from an initial state in which all genes are expressed at $e_{1/2}$. Note that, while there might be several stable or unstable fixed points of the system for a given genome and environment, our algorithm in practice always converges to a fixed point. We therefore define this point as the gene expression levels of that individual in that environment. A representative example of this computation is shown in the right-hand side panel of Figure 12.

5.2 Evolutionary Model

Equipped with a model of the coupling between DNA supercoiling and gene transcription at the whole-genome scale, we now embed it into an evolutionary framework. More precisely, we model the evolution of a population of individuals, each behaving as described in Subsection 5.1, which must simultaneously adapt to two distinct environments named A and B, as measured by an increase in fitness f (defined below) over time. Environment A induces DNA relaxation, with a supercoiling shift of $\delta\sigma_{env} = \delta\sigma_A = 0.01 > 0$, and environment B induces negative DNA supercoiling, with a supercoiling shift of $\delta\sigma_{env} = \delta\sigma_B = -0.01 < 0$. In order to represent adaptation to these environments, we assign genes in the individual's genomes to three categories, representing different target gene expression levels, in equal proportions: AB genes should be expressed in both environments, akin to housekeeping genes; A genes should be expressed in environment A but not in environment B; and, conversely, B genes should be expressed in environment B but not in environment A, both representing environment-specific genes, such as the pathogenic genes of *S. enterica* or *D. dadantii* (Cameron and Dorman, 2012; Hérault et al., 2014).

Fitness The fitness of an individual is computed using its gene expression levels in each of the two environments. Let $(e_A^{\mathrm{A}}, e_B^{\mathrm{A}}, e_{AB}^{\mathrm{A}})$ be the 3-dimensional vector representing the average gene expression level per gene type of an individual in environment A, and $(e_A^{\mathrm{B}}, e_B^{\mathrm{B}}, e_{AB}^{\mathrm{B}})$ be the average gene expression per gene type of this individual in environment B. Let $(\tilde{e}_A^{\mathrm{A}}, \tilde{e}_B^{\mathrm{A}}, \tilde{e}_{AB}^{\mathrm{A}})$ and $(\tilde{e}_A^{\mathrm{B}}, \tilde{e}_B^{\mathrm{B}}, \tilde{e}_{AB}^{\mathrm{B}})$ be the target expression values for each gene type in each environment, reflecting the gene type definitions presented above. For environment A, we set $\tilde{e}_A^{\mathrm{A}} = \tilde{e}_{AB}^{\mathrm{A}} = 1$, and $\tilde{e}_B^{\mathrm{A}} = e^{-m}$, which are respectively the maximal and minimal attainable gene expression levels in the model. Similarly, for environment B, we set $\tilde{e}_B^{\mathrm{B}} = \tilde{e}_{AB}^{\mathrm{B}} = 1$, and $\tilde{e}_A^{\mathrm{B}} = e^{-m}$. We can then compute the sum g of the squared error (or gap) between the mean and targeted expression levels for each gene type in each environment:

$$g = \sum_{i \in \{A,B,AB\}} \left(e_i^{\mathrm{A}} - \tilde{e}_i^{\mathrm{A}}\right)^2 + \sum_{i \in \{A,B,AB\}} \left(e_i^{\mathrm{B}} - \tilde{e}_i^{\mathrm{B}}\right)^2 \tag{5}$$

Finally, we define the fitness of the individual as $f = \exp(-k \cdot g)$, where k is a scaling factor representing the intensity of selection: as k increases, the difference in fitness, and hence in reproductive success, between individuals with different values of g also increases.

Evolutionary Algorithm We consider populations of N individuals, which reproduce in non-overlapping generations. At each generation, we first compute the fitness of each individual in that generation, based on its gene transcription levels in each environment (as described above). Then, in order to create the following generation, we draw N reproducers at random, proportionally to their fitness, and with replacement (meaning that a high-fitness individual can have several offspring) from the current generation. Finally, we create the offspring of each reproducer by randomly applying mutations to the genome of the reproducer, resulting in the new generation.

Mutational Operator: Genomic Inversions In order to model the evolution of genome organization, we use genomic inversions as the only mutational operator, so that genes might be reordered on the genome through series of inversions over evolutionary time. In particular, we do not include large-scale duplications or deletions, as these rearrangements might change the number of genes; in other words, we assume gene loss or duplication to be lethal mutations in this model. Note that translocations can be modeled as a series of well-chosen consecutive inversions, and are therefore implicitly present in our model.

In order to perform a genomic inversion, we choose a start point and an end point uniformly at random in the non-coding intergenic sections of the genome. This ensures that genes cannot be broken apart by inversions (remember that we assume that gene losses are lethal). Having chosen the ends of the inversion, we extract the DNA segment located between these points and reinsert it at the same position, but in the reverse orientation. The inversion thereby reverses the orientation of every gene inside the segment, but conserves the relative positions and distances between these genes. The intergenic sections at the boundaries of the inversion can however grow or shrink depending on the position of its start and end points, thereby allowing intergenic distances to change over evolutionary time. Note that the total amount of intergenic material, which is a parameter of the simulation (see next subsection), is itself kept constant by this operation.

Finally, when mutating an individual, we start by drawing the number of inversions to perform from a Poisson law of parameter $\lambda = 2$, meaning that the offspring of an individual will on average undergo two inversions. Then, we perform each inversion in succession as previously described, in order to obtain the final mutated offspring.

5.3 Experimental Setup

In order to conduct the simulations presented in the Results section, we let 30 independent populations of $N = 100$ individuals evolve for 1,000,000 generations. We initially seeded each population with 100 clones of a randomly generated individual with 60 genes, or 20 genes of each type (A, B and AB), using a different seed for each population. For the simulations presented in the Supplementary Material, we let 15 additional independent populations evolve for 250,000 generations, for each set of environmental perturbation values ($\sigma_A = 0.001$ and $\sigma_B = -0.001$, and $\sigma_A = 0.0001$ and $\sigma_B = -0.0001$ respectively).

The parameter values that we used are given in Table 1, and can be broadly grouped into genome-level parameters (gene length, intergenic distance, basal supercoiling level and supercoiling transmission distance) and promoter-level parameters (promoter opening threshold and effective thermal energy, crossover width). Both the genome-level parameters that describe the chromosome and the promoter-level parameters used to compute the transcriptional response to supercoiling were taken from averaged experimental values measured in *E. coli*. Note that the supercoiling transmission distance d_{max} is expected to be heterogeneous along a real chromosome; in our experiments, choosing larger values of d_{max} did not lead to qualitatively different results, but values smaller than 4 kb resulted in the loss of inhibition of genes A in environment B (data not shown). Also note that the torsional drag coefficient c is a new parameter that we introduce in this model to represent the influence of torsional drag on the local level of supercoiling. We have empirically chosen its value so that this effect is of the same magnitude as the other sources of supercoiling variations (i.e., environmental perturbations) in the model.

Parameter	**Symbol**	**Value**	**Reference**
Gene length	l	1,000 bp	Blattner (1997)
Initial intergenic distance	d_0	125 bp	Blattner (1997)
Supercoiling transmission distance	d_{max}	5,000 bp	Postow et al. (2004)
Basal supercoiling level	σ_{basal}	-0.066	Crozat et al. (2005)
Torsional drag coefficient	c	0.03	
Promoter opening threshold	σ_{opt}	-0.042	El Houdaigui et al. (2019)
Inverse effective thermal energy	m	2.5	El Houdaigui et al. (2019)
Crossover width	ε	0.005	El Houdaigui et al. (2019)

Table 1: Parameter values of the transcription-supercoiling coupling model used in the evolutionary simulations. The upper set of parameters is the genome-level parameters, the lower set the promoter-level parameters, both taken from the *E. coli* literature; the middle parameter is a new addition from our model.

5.4 Reproducibility and data availability

We implemented the simulation in Python, and optimized the computationally heavy parts using the `numba` package (Lam et al., 2015). The source code for the simulation, as well as the notebooks used for data analysis, are available online at the following address: `https://gitlab.inria.fr/tgrohens/evotsc`. Running the complete set of simulations took around 36 hours of computation on a server using a 24-core Intel Xeon E5-2620 v3 @ 2.40GHz CPU, with each replicate running on a single core and using approximately 300 MB of RAM. The data from the main run of the experiment is available online on the Zenodo platform, at the following address: `https://doi.org/10.5281/zenodo.7062757`. The supplementary data is available at the following address: `https://doi.org/10.5281/zenodo.7789492`.

References

Baba, T., Ara, T., Hasegawa, M., Takai, Y., Okumura, Y., Baba, M., Datsenko, K. A., Tomita, M., Wanner, B. L., and Mori, H. (2006). "Construction of *Escherichia Coli* K-12 In-frame, Single-gene Knockout Mutants: The Keio Collection". *Molecular Systems Biology* 2.1. DOI: `10.1038/msb4100050`.

Blattner, F. R. (1997). "The Complete Genome Sequence of Escherichia Coli K-12". *Science* 277.5331, pp. 1453–1462. DOI: `10.1126/science.277.5331.1453`.

Boulas, I., Bruno, L., Rimsky, S., Espeli, O., Junier, I., and Rivoire, O. (2023). "Assessing *in Vivo* the Impact of Gene Context on Transcription through DNA Supercoiling". *Nucleic Acids Research* 51.18, pp. 9509–9521. DOI: `10.1093/nar/gkad688`.

Brackley, C. A., Johnson, J., Bentivoglio, A., Corless, S., Gilbert, N., Gonnella, G., and Marenduzzo, D. (2016). "Stochastic Model of Supercoiling-Dependent Transcription". *Physical Review Letters* 117.1, p. 018101. DOI: `10.1103/PhysRevLett.117.018101`.

Brinza, L., Calevro, F., and Charles, H. (2013). "Genomic Analysis of the Regulatory Elements and Links with Intrinsic DNA Structural Properties in the Shrunken Genome of Buchnera". *BMC Genomics* 14.1, p. 73. DOI: `10.1186/1471-2164-14-73`.

Cameron, A. D. S. and Dorman, C. J. (2012). "A Fundamental Regulatory Mechanism Operating through OmpR and DNA Topology Controls Expression of Salmonella Pathogenicity Islands SPI-1 and SPI-2". *PLoS Genetics* 8.3, e1002615. DOI: `10.1371/journal.pgen.1002615`.

Champoux, J. J. (2001). "DNA Topoisomerases: Structure, Function, and Mechanism". *Annual Review of Biochemistry* 70.1, pp. 369–413. DOI: 10.1146/annurev.biochem.70.1.369.

Crombach, A. and Hogeweg, P. (2008). "Evolution of Evolvability in Gene Regulatory Networks". *PLoS Computational Biology* 4.7, e1000112. DOI: 10.1371/journal.pcbi.1000112.

Crozat, E., Winkworth, C., Gaffe, J., Hallin, P. F., Riley, M. A., Lenski, R. E., and Schneider, D. (2010). "Parallel Genetic and Phenotypic Evolution of DNA Superhelicity in Experimental Populations of Escherichia Coli". *Molecular Biology and Evolution* 27.9, pp. 2113–2128. DOI: 10.1093/molbev/msq099.

Crozat, E., Philippe, N., Lenski, R. E., Geiselmann, J., and Schneider, D. (2005). "Long-Term Experimental Evolution in Escherichia Coli . XII. DNA Topology as a Key Target of Selection". *Genetics* 169.2, pp. 523–532. DOI: 10.1534/genetics.104.035717.

de la Campa, A. G., Ferrándiz, M. J., Martín-Galiano, A. J., García, M. T., and Tirado-Vélez, J. M. (2017). "The Transcriptome of Streptococcus Pneumoniae Induced by Local and Global Changes in Supercoiling". *Frontiers in Microbiology* 8, p. 1447. DOI: 10.3389/fmicb.2017.01447.

Deng, S., Stein, R. A., and Higgins, N. P. (2004). "Transcription-Induced Barriers to Supercoil Diffusion in the *Salmonella Typhimurium* Chromosome". *Proceedings of the National Academy of Sciences* 101.10, pp. 3398–3403. DOI: 10.1073/pnas.0307550101.

Dorman, C. J. (2019). "DNA Supercoiling and Transcription in Bacteria: A Two-Way Street". *BMC Molecular and Cell Biology* 20.1, p. 26. DOI: 10.1186/s12860-019-0211-6.

Dorman, C. J. and Dorman, M. J. (2016). "DNA Supercoiling Is a Fundamental Regulatory Principle in the Control of Bacterial Gene Expression". *Biophysical Reviews* 8.3, pp. 209–220. DOI: 10.1007/s12551-016-0205-y.

El Hanafi, D. and Bossi, L. (2000). "Activation and Silencing of Leu-500 Promoter by Transcription-Induced DNA Supercoiling in the Salmonella Chromosome: Transcription-dependent Modulation of Leu-500 Promoter in topA Mutants". *Molecular Microbiology* 37.3, pp. 583–594. DOI: 10.1046/j.1365-2958.2000.02015.x.

El Houdaigui, B., Forquet, R., Hindré, T., Schneider, D., Nasser, W., Reverchon, S., and Meyer, S. (2019). "Bacterial Genome Architecture Shapes Global Transcriptional Regulation by DNA Supercoiling". *Nucleic Acids Research* 47.11, pp. 5648–5657. DOI: 10.1093/nar/gkz300.

Ferrandiz, M.-J., Martin-Galiano, A. J., Schvartzman, J. B., and de la Campa, A. G. (2010). "The Genome of Streptococcus Pneumoniae Is Organized in Topology-Reacting Gene Clusters". *Nucleic Acids Research* 38.11, pp. 3570–3581. DOI: 10.1093/nar/gkq106.

Forquet, R., Nasser, W., Reverchon, S., and Meyer, S. (2022). "Quantitative Contribution of the Spacer Length in the Supercoiling-Sensitivity of Bacterial Promoters". *Nucleic Acids Research* 50.13, pp. 7287–7297. DOI: 10.1093/nar/gkac579.

Forquet, R., Pineau, M., Nasser, W., Reverchon, S., and Meyer, S. (2021). "Role of the Discriminator Sequence in the Supercoiling Sensitivity of Bacterial Promoters". *mSystems* 6.4. DOI: 10.1128/mSystems.00978-21.

Gardner, T. S., Cantor, C. R., and Collins, J. J. (2000). "Construction of a Genetic Toggle Switch in Escherichia Coli". *Nature* 403.6767, pp. 339–342. DOI: 10.1038/35002131.

Geng, Y., Bohrer, C. H., Yehya, N., Hendrix, H., Shachaf, L., Liu, J., Xiao, J., and Roberts, E. (2022). "A Spatially Resolved Stochastic Model Reveals the Role of Supercoiling in Transcription Regulation". *PLOS Computational Biology* 18.9. Ed. by C. Zang, e1009788. DOI: 10.1371/journal.pcbi.1009788.

Grohens, T., Meyer, S., and Beslon, G. (2022). "A Genome-Wide Evolutionary Simulation of the Transcription-Supercoiling Coupling". *Artificial Life* 28.4, pp. 440–457. DOI: 10.1162/artl_a_00373.

Guo, M. S., Kawamura, R., Littlehale, M. L., Marko, J. F., and Laub, M. T. (2021). "High-Resolution, Genome-Wide Mapping of Positive Supercoiling in Chromosomes". *eLife* 10, e67236. DOI: 10.7554/eLife.67236.

Hérault, E., Reverchon, S., and Nasser, W. (2014). "Role of the LysR-type Transcriptional Regulator PecT and DNA Supercoiling in the Thermoregulation of *Pel* Genes, the Major Virulence Factors in *Dickeya Dadantii*: *Dickeya Dadantii* PecT Protein and Virulence Thermoregulation". *Environmental Microbiology* 16.3, pp. 734–745. DOI: 10.1111/1462-2920.12198.

Hsieh, L. S., Rouviere-Yaniv, J., and Drlica, K. (1991). "Bacterial DNA Supercoiling and [ATP]/[ADP] Ratio: Changes Associated with Salt Shock." *Journal of Bacteriology* 173.12, pp. 3914–3917. DOI: 10.1128/JB.173.12.3914-3917.1991.

Johnstone, C. P. and Galloway, K. E. (2022). "Supercoiling-Mediated Feedback Rapidly Couples and Tunes Transcription". *Cell Reports* 41.3, p. 111492. DOI: 10.1016/j.celrep.2022.111492.

Jovanovich, S. B. and Lebowitz, J. (1987). "Estimation of the Effect of Coumermycin A1 on Salmonella Typhimurium Promoters by Using Random Operon Fusions". *Journal of Bacteriology* 169.10, pp. 4431–4435. DOI: 10.1128/jb.169.10.4431-4435.1987.

Junier, I., Ghobadpour, E., Espeli, O., and Everaers, R. (2023). "DNA Supercoiling in Bacteria: State of Play and Challenges from a Viewpoint of Physics Based Modeling". *Frontiers in Microbiology* 14, p. 1192831. DOI: 10.3389/fmicb.2023.1192831.

Junier, I. and Rivoire, O. (2016). "Conserved Units of Co-Expression in Bacterial Genomes: An Evolutionary Insight into Transcriptional Regulation". *PLoS ONE* 11.5, e0155740. DOI: 10.1371/journal.pone.0155740.

Kim, S., Beltran, B., Imov, I., and Jacobs-Wagner, C. (2019). "Long-Distance Cooperative and Antagonistic RNA Polymerase Dynamics via DNA Supercoiling", p. 31.

Lam, S. K., Pitrou, A., and Seibert, S. (2015). "Numba: A LLVM-based Python JIT Compiler". *Proceedings of the Second Workshop on the LLVM Compiler Infrastructure in HPC - LLVM '15*. Austin, Texas: ACM Press, pp. 1–6. DOI: 10.1145/2833157.2833162.

Lenski, R. E. (2023). "Revisiting the Design of the Long-Term Evolution Experiment with Escherichia Coli". *Journal of Molecular Evolution*. DOI: 10.1007/s00239-023-10095-3.

Lenski, R. E., Rose, M. R., Simpson, S. C., and Tadler, S. C. (1991). "Long-Term Experimental Evolution in Escherichia Coli. I. Adaptation and Divergence During 2,000 Generations". *The American Naturalist* 138.6, pp. 1315–1341. JSTOR: 2462549.

Lilley, D. M. J., Chen, D., and Bowater, R. P. (1996). "DNA Supercoiling and Transcription: Topological Coupling of Promoters". *Quarterly Reviews of Biophysics* 29.3, pp. 203–225. DOI: 10.1017/S0033583500005825.

Liu, L. F. and Wang, J. C. (1987). "Supercoiling of the DNA Template during Transcription." *Proceedings of the National Academy of Sciences* 84.20, pp. 7024–7027. DOI: 10.1073/pnas.84.20.7024.

Marshall, D. G., Bowe, F., Hale, C., Dougan, G., and Dorman, C. J. (2000). "DNA Topology and Adaptation of Salmonella Typhimurium to an Intracellular Environment". *Phil. Trans. R. Soc. Lond. B* 355, pp. 565–574. DOI: 10.1098/rstb.2000.0598.

Martis B., S., Forquet, R., Reverchon, S., Nasser, W., and Meyer, S. (2019). "DNA Supercoiling: An Ancestral Regulator of Gene Expression in Pathogenic Bacteria?" *Computational and Structural Biotechnology Journal* 17, pp. 1047–1055. DOI: 10.1016/j.csbj.2019.07.013.

Menzel, R. and Gellert, M. (1987). "Modulation of Transcription by DNA Supercoiling: A Deletion Analysis of the Escherichia Coli gyrA and gyrB Promoters." *Proceedings of the National Academy of Sciences* 84.12, pp. 4185–4189. DOI: 10.1073/pnas.84.12.4185.

Meyer, S. and Beslon, G. (2014). "Torsion-Mediated Interaction between Adjacent Genes". *PLoS Computational Biology* 10.9, e1003785. DOI: 10.1371/journal.pcbi.1003785.

Muskhelishvili, G., Forquet, R., Reverchon, S., Meyer, S., and Nasser, W. (2019). "Coherent Domains of Transcription Coordinate Gene Expression During Bacterial Growth and Adaptation". *Microorganisms* 7.12, p. 694. DOI: 10.3390/microorganisms7120694.

Peter, B. J., Arsuaga, J., Breier, A. M., Khodursky, A. B., Brown, P. O., and Cozzarelli, N. R. (2004). "Genomic Transcriptional Response to Loss of Chromosomal Supercoiling in Escherichia Coli". *Genome Biology* 5, R87. DOI: 10.1186/gb-2004-5-11-r87.

Pineau, M., Martis B., S., Forquet, R., Baude, J., Villard, C., Grand, L., Popowycz, F., Soulère, L., Hommais, F., Nasser, W., Reverchon, S., and Meyer, S. (2022). "What Is a Supercoiling-Sensitive Gene? Insights from Topoisomerase I Inhibition in the Gram-negative Bacterium *Dickeya Dadantii*". *Nucleic Acids Research* 50.16, pp. 9149–9161. DOI: 10.1093/nar/gkac679.

Postow, L., Hardy, C. D., Arsuaga, J., and Cozzarelli, N. R. (2004). "Topological Domain Structure of the Escherichia Coli Chromosome". *Genes & Development* 18.14, pp. 1766–1779. DOI: 10.1101/gad.1207504.

Pruss, G. J. and Drlica, K. (1989). "DNA Supercoiling and Prokaryotic Transcription". *Cell* 56.4, pp. 521–523. DOI: 10.1016/0092-8674(89)90574-6.

Rhee, K. Y., Opel, M., Ito, E., Hung, S.-p., Arfin, S. M., and Hatfield, G. W. (1999). "Transcriptional Coupling between the Divergent Promoters of a Prototypic LysR-type Regulatory System, the ilvYC Operon of Escherichia Coli". *Proceedings of the National Academy of Sciences* 96.25, pp. 14294–14299. DOI: 10.1073/pnas.96.25.14294.

Sevier, S. A. and Hormoz, S. (2022). "Collective Polymerase Dynamics Emerge from DNA Supercoiling during Transcription". *Biophysical Journal* 121.21, pp. 4153–4165. DOI: 10.1016/j.bpj.2022.09.026.

Sobetzko, P. (2016). "Transcription-Coupled DNA Supercoiling Dictates the Chromosomal Arrangement of Bacterial Genes". *Nucleic Acids Research* 44.4, pp. 1514–1524. DOI: 10.1093/nar/gkw007.

Sutormin, D., Galivondzhyan, A., Musharova, O., Travin, D., Rusanova, A., Obraztsova, K., Borukhov, S., and Severinov, K. (2022). "Interaction between Transcribing RNA Polymerase and Topoi-

somerase I Prevents R-loop Formation in E. Coli". *Nature Communications* 13.1, p. 4524. DOI: 10.1038/s41467-022-32106-5.

Tobe, T., Yoshikawa, M., and Sasakawa, C. (1995). "Thermoregulation of virB Transcription in Shigella Flexneri by Sensing of Changes in Local DNA Superhelicity". *Journal of Bacteriology* 177.4, pp. 1094–1097. DOI: 10.1128/jb.177.4.1094-1097.1995.

Travers, A. and Muskhelishvili, G. (2005). "DNA Supercoiling — a Global Transcriptional Regulator for Enterobacterial Growth?" *Nature Reviews Microbiology* 3.2, pp. 157–169. DOI: 10.1038/nrmicro1088.

Visser, B. J., Sharma, S., Chen, P. J., McMullin, A. B., Bates, M. L., and Bates, D. (2022). "Psoralen Mapping Reveals a Bacterial Genome Supercoiling Landscape Dominated by Transcription". *Nucleic Acids Research* 50.8, pp. 4436–4449. DOI: 10.1093/nar/gkac244.

Webber, M. A., Ricci, V., Whitehead, R., Patel, M., Fookes, M., Ivens, A., and Piddock, L. J. V. (2013). "Clinically Relevant Mutant DNA Gyrase Alters Supercoiling, Changes the Transcriptome, and Confers Multidrug Resistance". *mBio* 4.4. DOI: 10.1128/mBio.00273-13.

Yus, E., Lloréns-Rico, V., Martínez, S., Gallo, C., Eilers, H., Blötz, C., Stülke, J., Lluch-Senar, M., and Serrano, L. (2019). "Determination of the Gene Regulatory Network of a Genome-Reduced Bacterium Highlights Alternative Regulation Independent of Transcription Factors". *Cell Systems* 9.2, 143–158.e13. DOI: 10.1016/j.cels.2019.07.001.